DISTYRYL-BORADIAZAINDACENES AS RED AND NIR SWITCHES

A THESIS SUBMITTED TO

THE GRADUATE SCHOOL OF NATURAL AND APPLIED SCIENCES

OF

MIDDLE EAST TECHNICAL UNIVERSITY

BY

G. CEYDA İŞBAŞAR

IN PARTIAL FULFILLMENT OF THE REQUIREMENTS

FOR

THE DEGREE OF MASTER OF SCIENCES

IN

CHEMISTRY

JUNE 2007

Approval of the Graduate School of Natural and Applied Sciences

_____
Prof. Dr. Canan Özgen
Director

I certify that this thesis satisfies all requirements as a thesis for the degree of Master of Science.

_____
Prof. Dr. Ahmet Önal
Head of Department

This is to certify that we have read this thesis and in our opinion, it is fully adequate, in scope and quality, as a thesis for the degree of Master of Science.

_____
Prof. Dr. Engin U. Akkaya
Supervisor

Examining Committee Members

Prof. Dr. İdris M. Akhmedov	(METU, CHEM)	_____
Prof. Dr. Engin U. Akkaya	(METU, CHEM)	_____
Prof. Dr. İnci Gökmen	(METU, CHEM)	_____
Assoc. Prof. Dr. Özdemir Doğan	(METU, CHEM)	_____
Asst. Prof. Neslihan Şaki	(Kocaeli Univ., CHEM)	_____

I hereby declare that all information in this document has been obtained and presented in accordance with academic rules and ethical conduct. I also declare that, as required by these rules and conduct, I have fully cited and referenced all material and results that are not original to this work.

Name, Last name : G. CEYDA İŞBAŞAR
Signature :

ABSTRACT

DISTYRYL-BORADIAZAINDACENES AS RED AND NIR SWITCHES

İşbaşar, G. Ceyda
M.S., Department of Chemistry
Supervisor: Engin U. Akkaya

June 2007, 61 pages

Two novel distyryl-boradiazaindacene dyes with dimethylaminophenyl and pyridyl appendages, display opposite spectral shifts on protonation with trifluoroacetic acid in organic solvents. This bidirectional switching of the dyes can be shown to be directly related to ICT donor and acceptor characteristics of the dyes. Thus, it has been demonstrated that the switching behavior of the red to NIR emitting dyes can be altered by simple structural modifications.

Keywords: distyryl-boradiazaindacene, Internal Charge Transfer (ICT), bidirectional switching.

ÖZ

KIRMIZI VE YAKIN KIZILÖTESİ EMİSYONU OLAN DİSTİRİL-BORADİAZAİNDASENLER

İşbaşar, G. Ceyda
Yüksek Lisans, Kimya Bölümü
Tez Yöneticisi: Engin U. Akkaya

Haziran 2007, 61 sayfa

Dimetilaminofenil- ve piridil- grupları içeren iki yeni distiril-boradiazaindasen boyar maddeleri organik çözücülerde TFA (trifluoroasetik asit) ile protone edildikleri zaman, ters yönde spektral kayma göstermektedirler. Emisyonun iki yönlü modifikasyonu, boyar maddelerin yapisinda bulunan grupların İYT donor ya da akseptör niteliklerine bağlanmıştır. Bu durumda, kırmızı ile yakın kızılötesi emisyona sahip olan boyar maddelerin spektral karakterlerinin basit yapısal modifikasyonlar ile değiştirilebileceği gösterilmiştir.

Anahtar Kelimeler: distiril-boradiazaindasen, İçsel Yük Transferi (İYT), iki yönlü şalter.

To my parents…

ACKNOWLEDGEMENT

This thesis was carried out at the Chemistry Department of Middle East Technical University during the years 2005-2007.

I am so greatful to my supervisor Prof. Dr. Engin U. Akkaya for his guidance, support, patience and advices throughout this research as well as his unlimited knowledge and experiences that I benefited greatly.

I would like to thank Alex Siemiarczuk for the lifetime measurements and Leyla Yıldırım for X-ray analysis.

I would like to express my special thanks to my parents, Oğuz and Güzin, my sister Ceren and her husband Fikri for their love, support, encouragement, understanding, trust and the other things that I do not mention.

I sincerely thank all my close friends for their endless friendship.

I wish also thank the always helpful staff in the Chemistry Department.

Finally, I thank all my group members.

TABLE OF CONTENTS

LIST OF TABLES

LIST OF FIGURES

LIST OF ABBREVIATIONS

AIBN: 2,2'-Azobis(2-methylpropionitrile)

AAS: Atomic Absorption Spectroscopy

AES: Atomic Emission Spectroscopy

BF_3OEt_2: Boron trifluoride-diethyl etherate

BODIPY: 4,4-difluoro-4-bora-3a,4a-diaza-*s*-indacene

DNA: Deoxyribonucleic acid

HOMO: Highest Occupied Molecular Orbital

ICT: Internal Charge Transfer

LUMO: Lowest Unoccupied Molecular Orbital

NMR: Nuclear Magnetic Resonance Spectroscopy

NBD: 7-nitro-2,1,3-benzoxadiazol-4-yl

NIR: Near infrared

NBS: N-Bromosuccinimide

PET: Photoinduced Electron Transfer

TFA: Trifluoroacetic acid

UV/Vis: Ultra-Violet/Visible

CHAPTER 1

INTRODUCTION

1.1. Supramolecular Chemistry

Prof. Jean-Marie Lehn[*] established the modern notion of supramolecular chemistry in 1978, which can be briefly described as "the chemistry of molecular assemblies and of the intermolecular bond." His pioneering work on supramolecular chemistry inspired scientists across chemical sciences. To this date, several phrases were used to define this fascinating field of chemistry such as "chemistry beyond the molecule," "the chemistry of the non-covalent bond," and "non-molecular chemistry" or even "Lego chemistry" **[1-3]** (Figure 1). Various intermolecular forces may act to associate two or molecular species such as electrostatic interaction, hydrogen bonding, π-π stacking interaction, van der Waals forces, or hydrophobic effects. These interactions form organized entities of higher complexity **[4]**.

Supramolecular chemistry is highly interdisciplinary field of science covering the chemical, physical, and biological features of the chemical species of greater complexity than molecules themselves. Its roots extend into organic chemistry and the synthetic procedures for molecular construction, into coordination chemistry and metal ion-ligand

[*] Nobel Laureate in Chemistry (1987)

complexes, into physical chemistry and the experimental and theoretical studies of interactions, into biochemistry and the biological processes that all start with substrate binding and recognition, into materials science and the mechanical properties of solids **[5]**. In conclusion, it can be said that supramolecular chemistry is inspired by the biological processes and the chemists are trying to mimic these in molecular level.

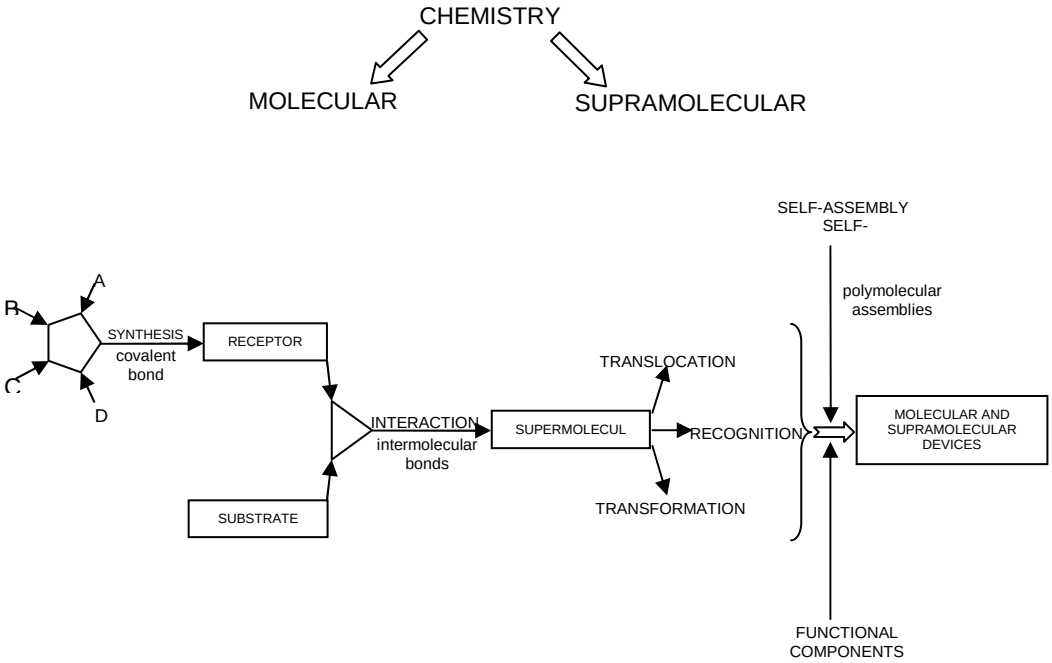

Figure 1 The science of chemistry according to Jean-Marie Lehn and the schematic representation of how supramolecular devices are built by bottom-up approach **[5]**.

Essentially, the reciprocal interactions of molecules or molecular entities with discrete properties are related to the supramolecular chemistry. Non-covalent interactions mainly form these reciprocal interactions. Supramolecules are assemblies in which a number of components come together spontaneously to make a larger entity with properties derived from its components.

1.2. Intermolecular Forces

Intermolecular forces are the non-covalent interactions holding the molecules together in supramolecular chemistry. Intermolecular forces include:

- Electrostatic interactions (ion-ion, ion-dipole, dipole-dipole);
- H-bonding;
- π-π stacking interactions;
- Dispersion and induction forces (van der Waals forces);
- Hydrophobic or solvatophobic effects.

1.2.1. Electrostatic Interactions

Electrostatic interactions depend on the Coulombic attractions caused by opposite charges. (Figure 2) Electrostatic interactions are seen between ion-ion, ion dipole, or dipole-dipole. Ion-ion interactions are non-directional, though for the ion-dipole interactions dipole must be properly aligned for most favorable binding efficiency **[4]**.

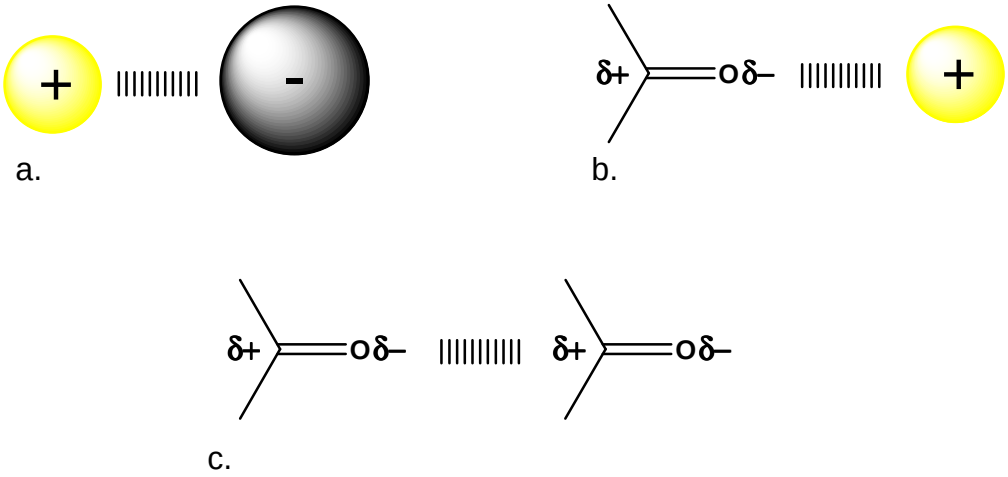

Figure 2 Electrostatic interactions; a. ion-ion, b. ion-dipole, c. dipole-dipole

1.2.2. H-Bonding

H-bonded complexes are undoubtedly the most important and numerous noncovalent complexes. For instance, the interactions in water molecule are one of the most crucial forces found in nature. (Figure 3) They give water its unique properties that are so important to life on earth. Hydrogen bonding occurs when a hydrogen atom is covalently bonded to a small highly electronegative atom such as nitrogen, oxygen, or fluorine. The result is a dipolar molecule. The hydrogen atom has a partial positive charge δ+ and can interact with another highly electronegative atom in an adjacent molecule (again N, O, or F). This results in a stabilizing interaction that binds the two molecules together.

H-bonds determine the structure of bio-macromolecules such as DNA and proteins and play a key role in the important biophysical process of

molecular recognition (Figure 4). H-bonding is also a pattern commonly used in supramolecular synthesis **[6]**.

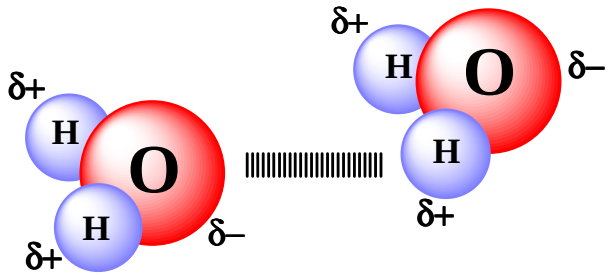

Figure 3 An example for H-Bonding between oxygen and hydrogen atoms

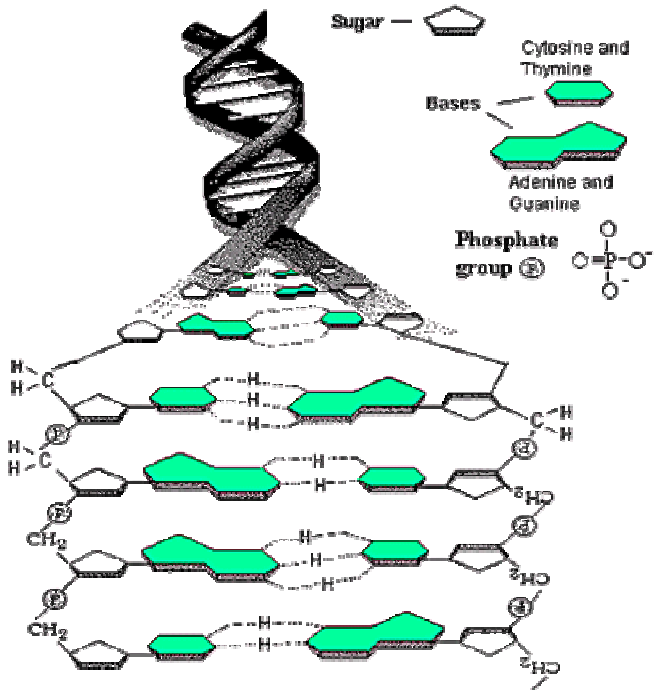

Figure 4 H-bonding between Adenine (or Guanine) and Thymine (or Cytosine) molecules in DNA[†]

[†] DNA structure was taken from www.accessexcellence.org/AB/GG/dna_molecule.html

1.2.3. π-π Stacking Interactions

π-π Stacking interactions are observed between aromatic rings, regularly in situations where one is relatively e⁻-deficient and other is e⁻-rich. Two general types of π-π stacking exist: face-to-face and edge-to-face (Figure 5). Edge-to-face π-π stacking interactions may be regarded as weak forms of H-bonds between the slightly e⁻-deficient hydrogen atoms of one aromatic ring and the electron rich π-cloud of another **[7]**.

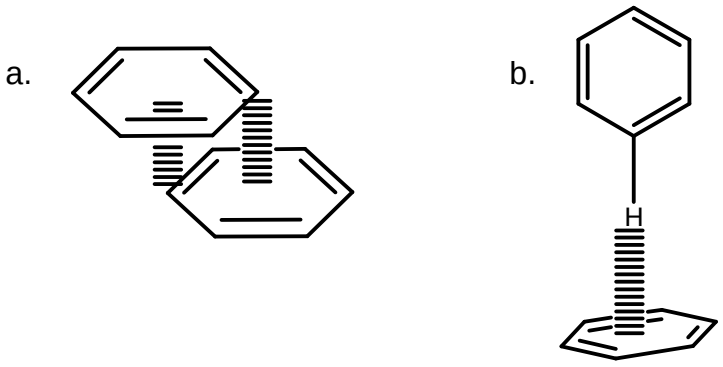

Figure 5 Common types of π-π stacking; a. face-to-face b. edge-to-face

1.2.4. Van der Waals Forces

Van der Waals interactions arise from the polarization of an e⁻-cloud by the nearness of an adjacent nucleus, resulting in a weak electrostatic interaction. They are nondirectional and for this reason have only limited scope in the design of specific hosts for selective complexation

of particular guests. In supramolecular chemistry, van der Waals forces are mainly crucial in construction of “inclusion” compounds in which small, classically organic molecules are loosely incorporated within molecular cavities or crystalline lattices. Rigorously, van der Waals interactions may be divided into dispersion (London) and induction terms. The dispersion interaction is the attractive part that results from the interactions between fluctuating multipoles in neighboring molecules. The attraction decreases extremely fast with distance and is additive with every bond in the molecule contributing to the overall interaction energy. The exchange-repulsion defines molecular shape and balance dispersion at short range **[7]**.

1.2.5. Hydrophobic Effects

Hydrophobic effects generally relate to the exclusion from polar solvent, mainly water, of large particles or those that are weakly solvated. Fundamentally, the water molecules are attracted strongly to one another causing a natural aggregation of other species as they force out of the way of the strong intersolvent interactions. This can produce effects resembling attraction between one organic molecule and another. Hydrophobic effects may be composed of two energetic components: enthalpic and entropic. The enthalpic hydrophobic effect includes the stabilization of water molecules that are driven from a host cavity upon guest binding. Since host cavities are often hydrophobic, intracavity water does not interact strongly with the host walls and is therefore of high energy. It is stabilized by interactions with other water molecules, in accordance with release into the bulk solvent. The entropic hydrophobic effect arises from the fact that the presence of two molecules in solution (host and guest) creates two “holes” in the

structure of bulk water. Formation of a complex by combining host and guest causes less disruption to the solvent structure and therefore an entropic gain **[7]**.

1.3. Luminescence Process

The emission of photons from electronically excited states is the luminescence. Luminescence is composed of two types, depending upon the nature of the ground and the excited states. In a singlet state, the electron in the higher-energy orbital has the opposite spin orientation as the second electron in the lower orbital. In a triplet state these electrons have the same spin orientation. Coming back to the ground state from an excited singlet state does not necessitate an electron to change its spin orientation. On the other hand a change in spin orientation is necessary for a triplet state to return to the singlet ground state. Fluorescence is the emission which results from the return to the lower orbital of the paired electron. Such transitions are quantum mechanically “allowed” and emissive rates are typically near 10^8 sec^{-1}. These high emissive rates result in fluorescence lifetimes near 10^{-8} sec or 10 nsec **[8]**.

1.4. Jablonski Diagram

The energy level diagram recommended by A. Jablonski illustrates adequately the absorption and emission of light. S_0, S_1 and S_2 represent the ground, first electronic and second electronic states, respectively.

The fluorophores may present at each of these electronic energy levels in a number of vibrational energy levels, represented by 0, 1, 2… (Figure 6) **[8]**.

Just after the absorption of light a number of processes generally take place. A fluorophore is typically excited to some higher vibrational level of S_2. In general it rapidly relaxes to the lowest vibrational level of S_2 through collisions between the molecules of the excited species and those of the solvent. This is said to be *vibrational relaxation* and generally occurs in 10^{-12} sec or less. Additionally another process called *internal conversion* takes place when two electronic energy levels are sufficiently close therefore an overlap in vibrational energy levels is observed. *Fluorescence* is the emission from the lowest vibrational energy level of excited state to any vibrational energy level of ground state. When the lowest singlet vibrational state overlaps one of the upper triplet vibrational levels, *intersystem crossing* process is observed in which the spin of an excited electron is reversed. After intersystem crossing to an triplet state, further deactivation can occur by phosphorescence. Transition from triplet excited state to the singlet ground state is forbidden, and as a result the lifetimes range from milliseconds to seconds **[8, 9]**.

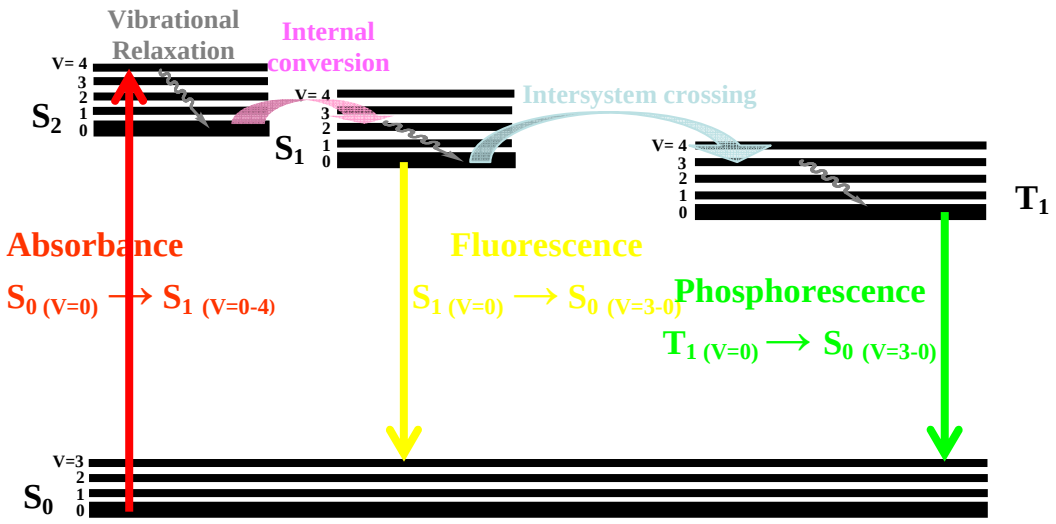

Figure 6 Jablonski Diagram describing luminescence processes

1.5. Distinguishing Features of Fluorescence

1.5.1. Stokes' Shift

A shift in spectra of absorption and emission is observed due to the loss of energy through radiationless relaxations (Figure 7). The rapid decay to the lowest vibrational level S_1 is the most common reason for the Stokes' Shift. Moreover, further loss of vibrational energy can be observed following the decay to excited vibrational levels of S_0 ($S_{1\ (V=0)} \rightarrow S_{0\ (V=3\text{-}1)}$). Additionally, Stokes' Shift can be displayed due to solvent effects and excited state reactions **[8]**.

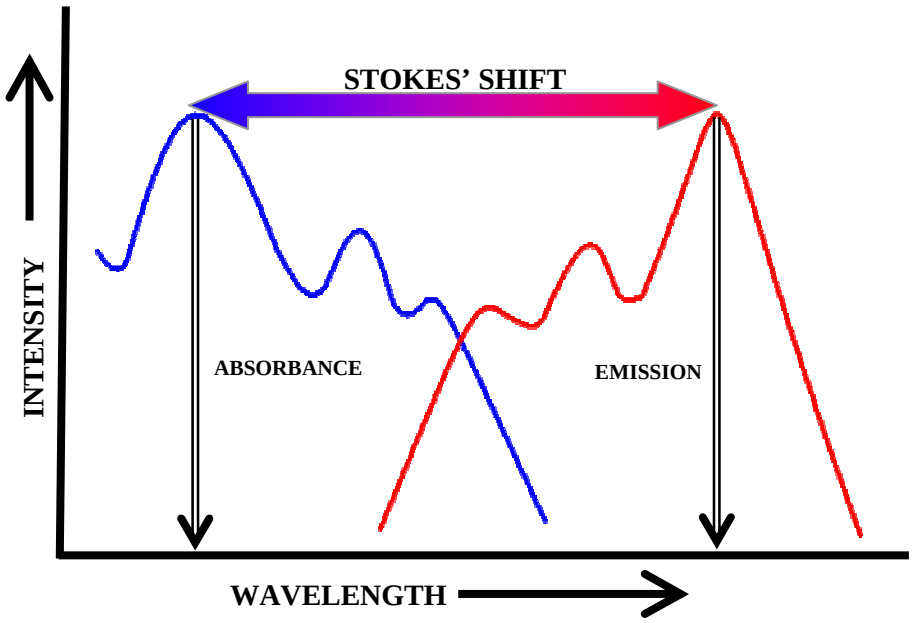

Figure 7 Stokes' shift

1.5.2. Steadiness of the Emission Spectrum with Excitation Wavelength

After the excitation to higher electronic and vibrational levels, the excess energy is readily released leaving the molecule in the lowest vibrational level of S_1. As a result of this rapid relaxation, emission spectrum is generally independent of the excitation wavelength. Exceptions present, such as azulene, which may emit from both S_2 and S_1 **[8]**.

1.5.3. Mirror Image Rule

Fluorescence emission spectrum generally is observed as the mirror image of the absorption spectrum, especially for the transition from S_0 to S_1. This symmetric nature of these spectra results from the same transitions being involved in both absorption and emission, and the similarities among the vibrational energy levels of S_0 and S_1. According to the Franck-Condon principle, all electronic transitions are vertical. Consequently, if a particular transition probability between the 0 and 2nd vibrational levels is largest in absorption, the reciprocal transition is also most probable in emission (Figure 8). Many exceptions to the mirror image rule are also observed. These exceptions are a result of the different geometric arrangement of nuclei in the excited state when compared to the ground state. Excited state reactions can also cause exceptions to the mirror image rule **[8]**.

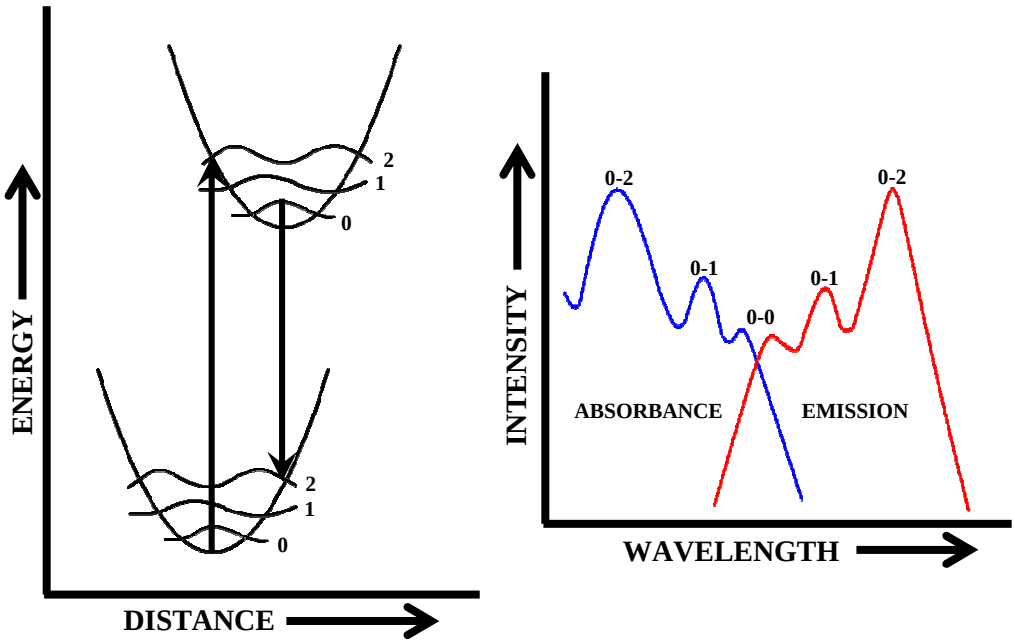

Figure 8 Franck-Condon principle and mirror image rule

1.6. Quantum Yield

The quantum yield, or quantum efficiency, is the ratio of the number of molecules that exhibit luminescence to the total number of excited molecules. The quantum efficiency for highly fluorescent molecules can approach unity. On the other hand, for molecules that do not display fluorescence appreciably the quantum efficiency may approach zero. The fluorescence quantum yield ϕ for a compound can be determined by the relative rate constants k_x for the processes by which the lowest excited singlet state is deactivated; k_f, k_i, k_{ec}, k_{ic}, k_{pd}, k_d. These relationships can be expressed by Equation 1 **[9]**.

$$\phi = \frac{k_f}{k_f + k_i + k_{ec} + k_{ic} + k_{pd} + k_d}$$

Equation 1 Quantum yield

k_f: fluorescence rate constant
k_i: rate constant of intersystem crossing
k_{ec}: rate constant of external conversion
k_{ic}: rate constant of internal conversion
k_{pd}: predissociation rate constant
k_d: dissociation rate constant

1.7. Effects of Some Parameters on Fluorescence

1.7.1. Structure

Fluorescence found in molecules containing aromatic functional groups is the most intense and the most useful. The majority of unsubstituted aromatic hydrocarbons have fluorescence in solution. The quantum efficiency generally enhances with the number of rings and their degree of condensation. Molecules containing aliphatic and alicyclic carbonyl structures or highly conjugated double-bond structures may also display fluorescence. The simple heterocyclics, such as pyridine, furan, thiophene, and pyrrole (Figure 9), do not display fluorescence; on the other hand, fused-ring structures, such as quinoline, isoquinoline, and indole (Figure10), usually do **[9]**.

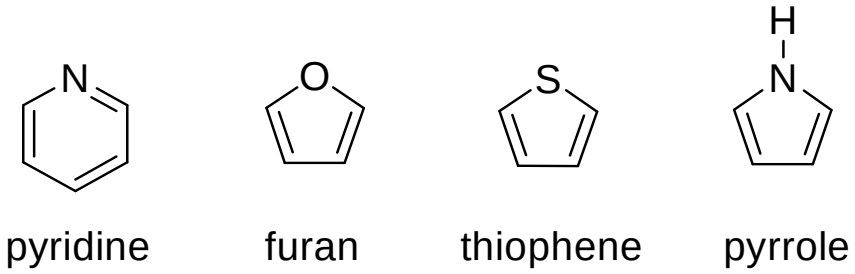

Figure 9 Simple heterocyclics

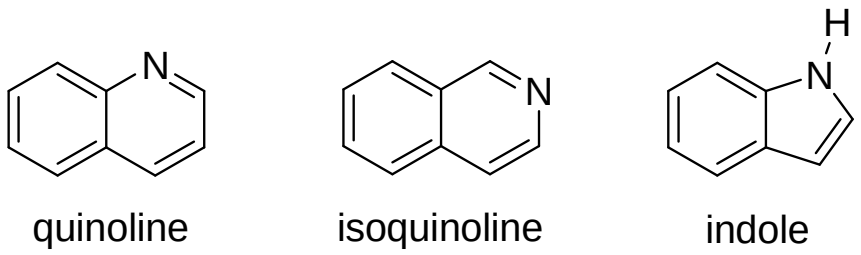

Figure 10 Fused-ring structures with nitrogen heterocyclics

1.7.2. Structural Rigidity

Molecules having rigid structures display fluorescence better. Lack of rigidity in a molecule probably results in an enhanced internal conversion rate and a consequent increase in the likelihood for radiationless deactivation. The quantum efficiencies for fluorene and biphenyl are nearly 1.0 and 0.2, respectively (Figure 11). The difference in behavior appears to be largely a result of the increased rigidity supplied by the bridging methylene group in fluorene **[9]**.

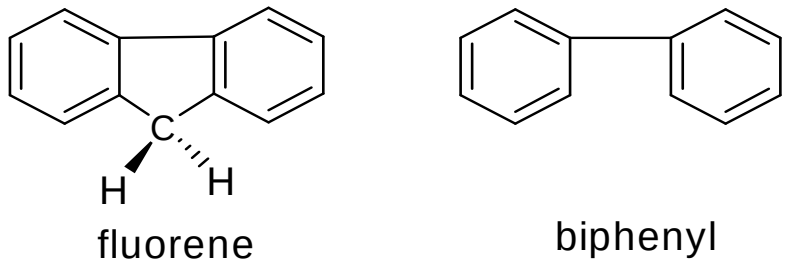

Figure 11 Effect of rigidity on fluorescence

1.7.3. Temperature and Solvent

The quantum efficiency of fluorescence generally diminishes with increasing temperature due to increasing frequency of collisions at high temperatures improves the probability for deactivation by external conversion. A decrease in solvent viscosity also increases the likelihood of external conversion and leads to the same result. The fluorescence of a molecule is decreased by solvents containing heavy atoms or other solutes with such atoms in their structure. The effect is similar to that which occurs when heavy atoms are substituted into fluorescence compounds; orbital spin interactions result in an increase in the ratio of triplet formation and a corresponding decrease in fluorescence **[9]**.

1.7.4. Acidity (pH)

The fluorescence of aromatic compounds that contain acidic or basic substituents depends on pH. The wavelength and the emission intensity of ionized and nonionized forms of such compounds show difference. The changes in emission are resulted from the differing number of resonance species that are associated with the acidic and basic forms of the molecule. For instance, aniline has several resonance forms whereas anilinium has one (Figure 12). These additional resonance forms make the first excited state of the molecule more stable; therefore the fluorescence is observed in the ultraviolet region **[9]**.

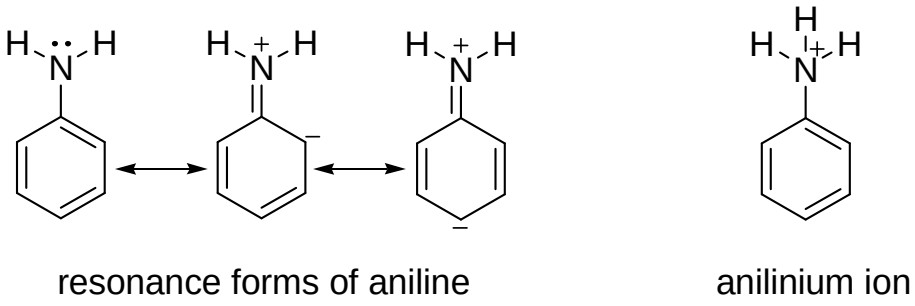

Figure 12 Structures of resonance forms of aniline and anilinium ion

1.7.5. Dissolved Oxygen

Fluorescence intensity decreases in the presence of dissolved oxygen due to the quenching resulted from the paramagnetic properties of oxygen which leads to intersystem crossing and conversion of excited molecules to the triplet state. Also other paramagnetic species causes quenching of fluorescence **[18]**.

1.7.6. Concentration

Fluorescence is also concentration dependent. For the absorbance (A) less than 0.05, there is a direct proportion between the fluorescence power (F) and the concentration (c) (Equation 2).

$$F = 2.3K'\varepsilon bcP_0$$

Equation 2 Relation between fluorescence and concentration for low absorbance

K': a constant depends on the quantum efficiency of the fluorescence process.

ε: molar absorptivity

b: length of the medium

P_0: power of the beam incident upon the solution

Therefore, for low concentrations the plot of the fluorescence power versus concentration should be linear. When the concentration becomes great enough so that the absorbance is larger than 0.05, linearity is lost; fluorescence power then lies below an extrapolation of the straight-line plot **[9]**.

Self-quenching and self-absorption are also responsible for negative departures from linearity at high concentration. Self-quenching is caused by collisions between excited molecules, thus radiationless energy transfer occurs. Self-quenching can be expected to increase with concentration due to the greater possibility of collisions occurring. Self-absorption occurs when the wavelength of emission overlaps an absorption peak; fluorescence is then decreased as the emission passes through the solution and is reabsorbed by other fluorescent molecules. Consequently, these effects cause a maximum in the plot of fluorescence versus concentration **[9]**.

1.8. Fluorescent Cation Sensors

Chemists, biologists, biochemists and environmentalists are deeply interested in detecting cations due to their functions in biological systems, treating some diseases and their toxic effects. Although many analytical method exists, such as flame photometry, atomic absorption spectrometry, ion sensitive electrodes, electron microprobe analysis, neutron activation analysis, to detect cations, fluorescent sensors possess advantages in terms of sensitivity, selectivity, response time, local observation **[10]**.

Flouroionophore is the fluorescent sensor composed of a fluorophore linked to an ionophore. A fluoroionophore could be either spaced or integrated (Figure 13) **[10]**.

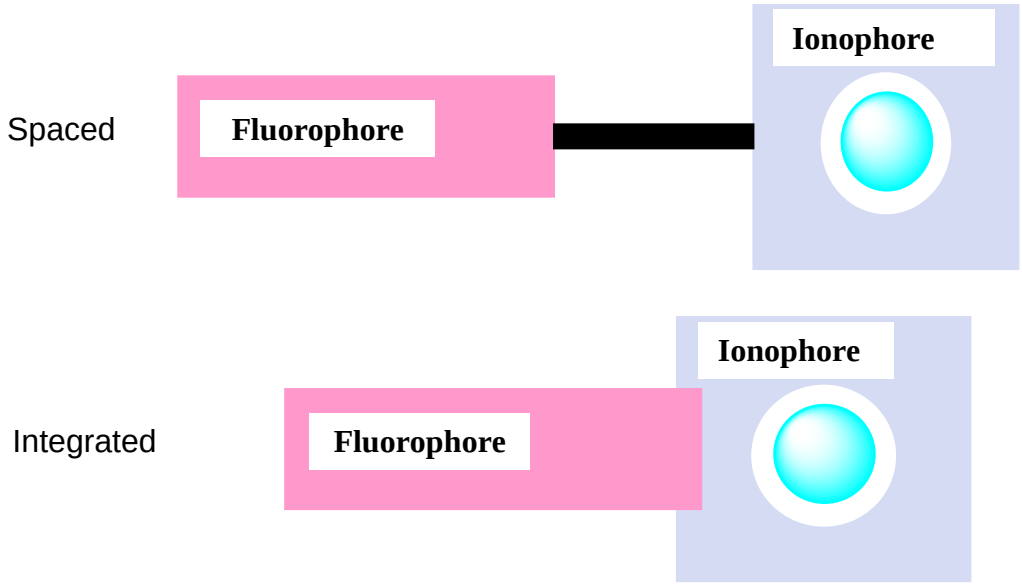

Figure 13 Spaced and integrated forms of the fluoroionophore

The *signaling moiety* is the signal transducer component of the fluoroionophore and converts the information into an optical signal expressed as the changes in the photophysical charecteristics of the fluorophore. The recognition moiety is responsible for selectivity and efficiency of binding which depend on the ligand topology, on the characteristics of the cation (ionic radius, charge, coordination number, hardness, etc.), and on the nature of the solvent (Figure 14) **[10]**.

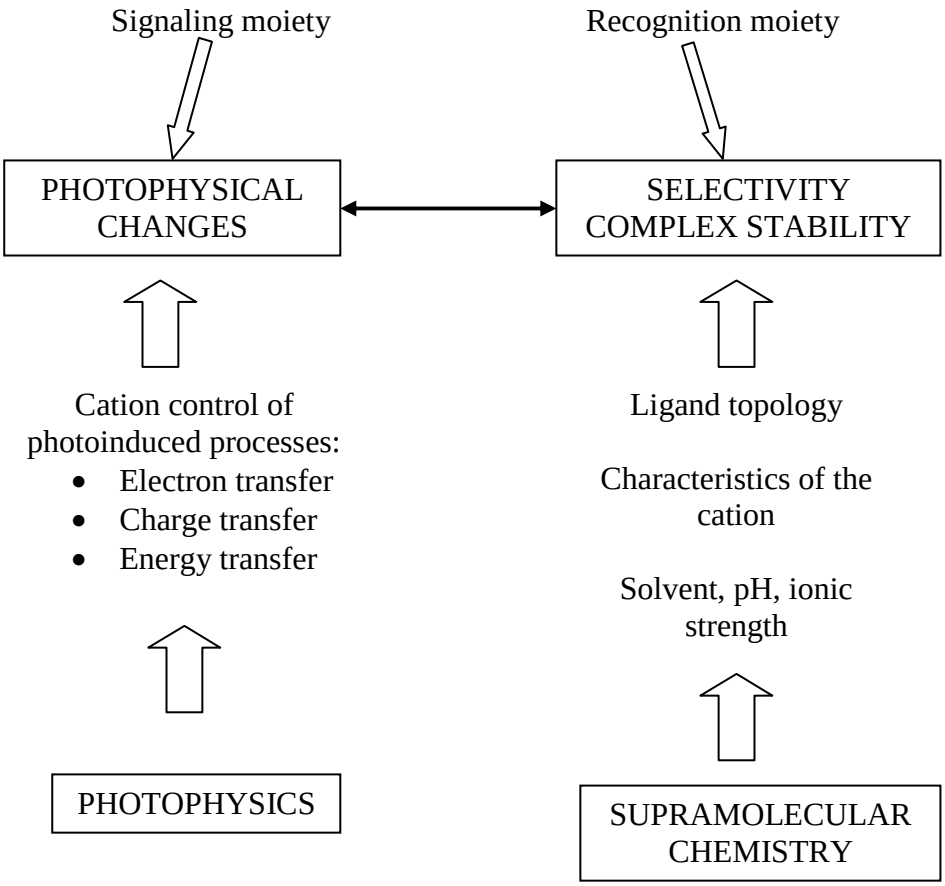

Figure 14 Signaling and recognition moiety

A classification according to the nature of the photoinduced process which is responsible for photophysical changes upon cation binding is done while designing the fluorescent sensors for cations.

1.8.1. Fluorescent Sensors with PET (Photoinduced Electron Transfer) Systems

Such sensors are composed of two parts, a fluorophore that is responsible for the excitation and emission and a receptor that is responsible for complexation and decomplexation, connected to each other by a spacer **[11]**. An electron of the highest occupied molecular orbital (HOMO) is excited to the lowest unoccupied molecular orbital (LUMO) upon the fluorophore excitation. This enables PET from the HOMO of the donor that is free from cation to that of the fluorophore. Hence the fluorescence results in quenching. The redox potential of the donor is increased upon cation binding; therefore the relevant HOMO becomes lower in energy than that of the fluorophore. As a result PET becomes impossible and quenching of the fluorescence is suppressed. This means that cation binding to the donor increases the fluorescence intensity (Figure 15) **[10]**.

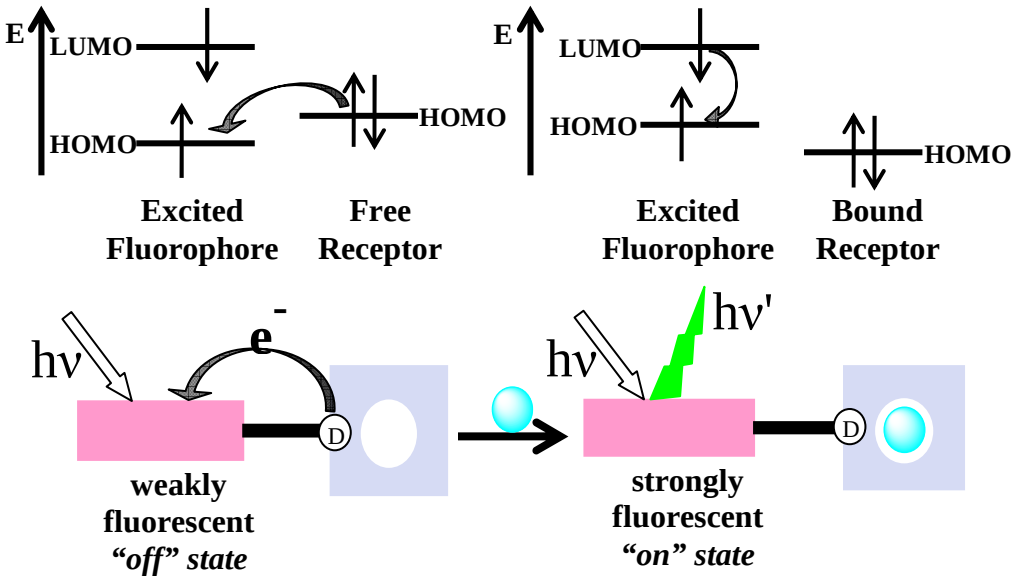

Figure 15 Mechanism of photoinduced electron transfer

1.8.2. Fluorescent Sensors with ICT (Internal Charge Transfer) Systems

In contrast with PET systems, a fluorophore can be directly integrated with a receptor **[12]**. This receptor can be either an electron donating group or an electron accepting group. In the case of the electron donating group, interaction with a cation reduces the electron donating ability of this group. The excited state is more strongly destabilized by the cation than the ground state. A blue shift (shift to left) of the absorption spectrum is desired due to the reduction of conjugation. The fluorescence spectrum is in principle shifted in the same direction as that of the absorption spectrum. Conversely, when a cation interacts with the electron acceptor group, electron withdrawing ability of this group increases. The excited state is more stabilized by the cation than the ground state. A red shift (shift to right) of the absorption and emission spectra is expected (Figures 16-17) **[10]**.

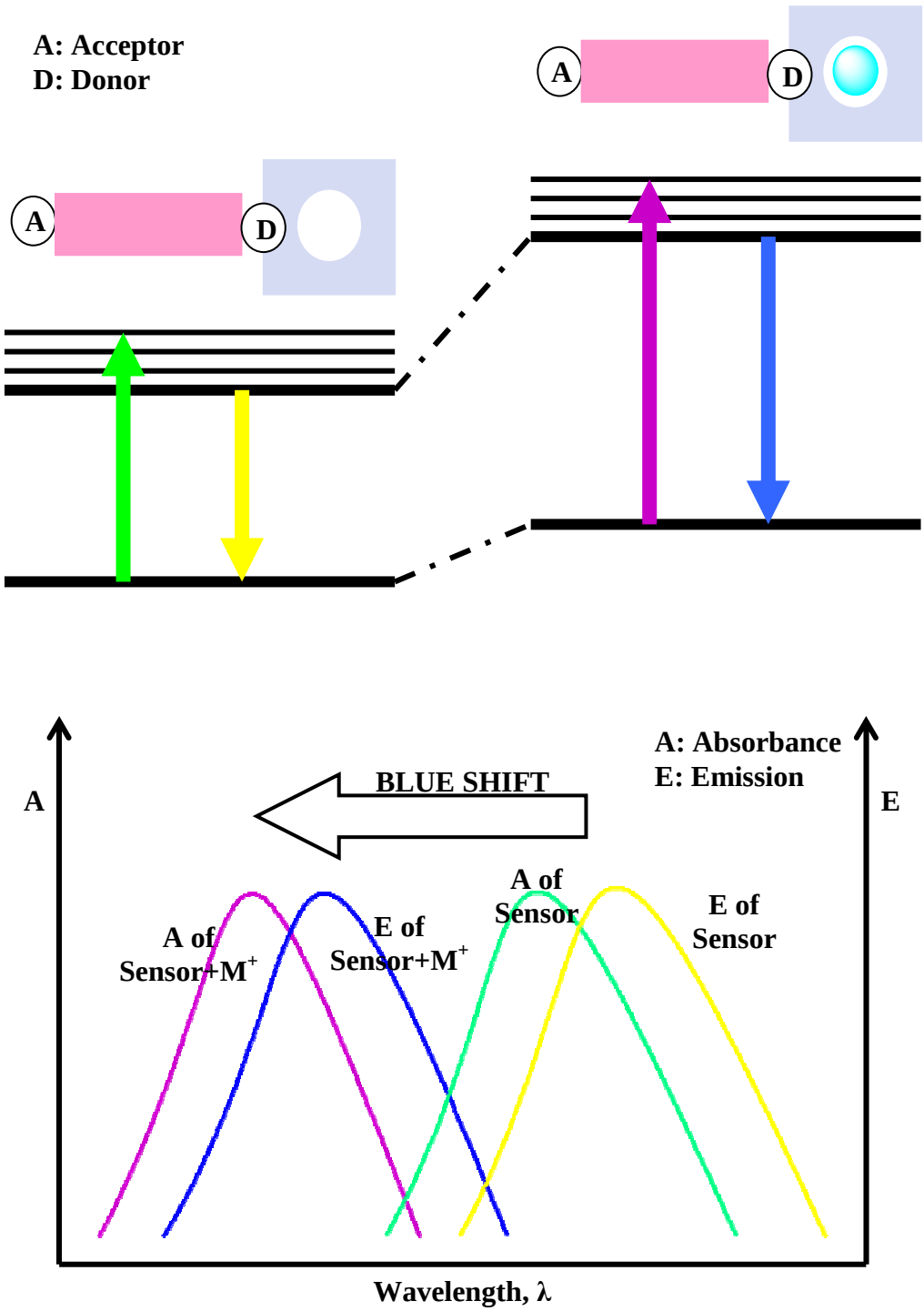

Figure 16 Schematic explanation of the spectral displacements of fluorescent ICT sensors that are caused by the interaction between a cation and an electron donating group

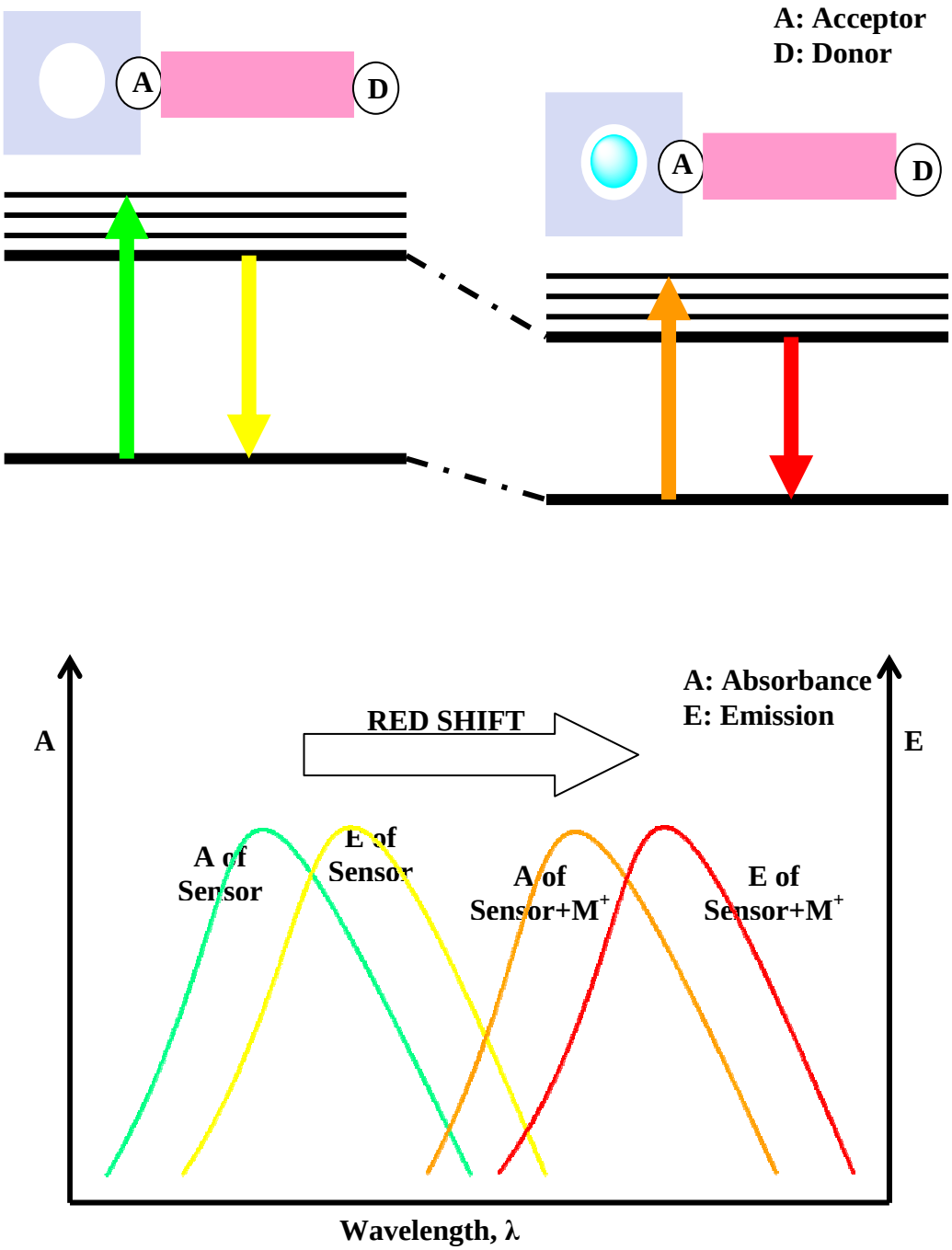

Figure 17 Schematic explanation of the spectral displacements of fluorescent ICT sensors that are caused by the interaction between a cation and an electron acceptor group

1.8.2.1. Fluorescent sensors in which cation binds to the electron donating group

These fluorescent sensors can be classified according to the chemical structure of the electron donating group.

- Crown-containing fluorescent ICT sensors
- Chelating fluorescent ICT sensors
- Cryptand-based fluorescent ICT sensors
- Calixarene-based fluorescent ICT sensors (Figure 18) **[10]**

1.8.2.2. Fluorescent sensors in which cation binds to the electron accepting group

Similarly, these fluorescent sensors can be classified according to the chemical structure of the electron accepting group. (Figure 19) **[10]**

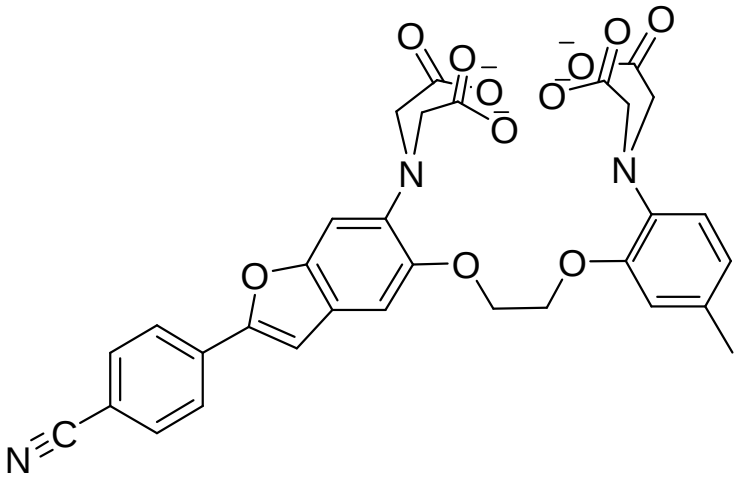

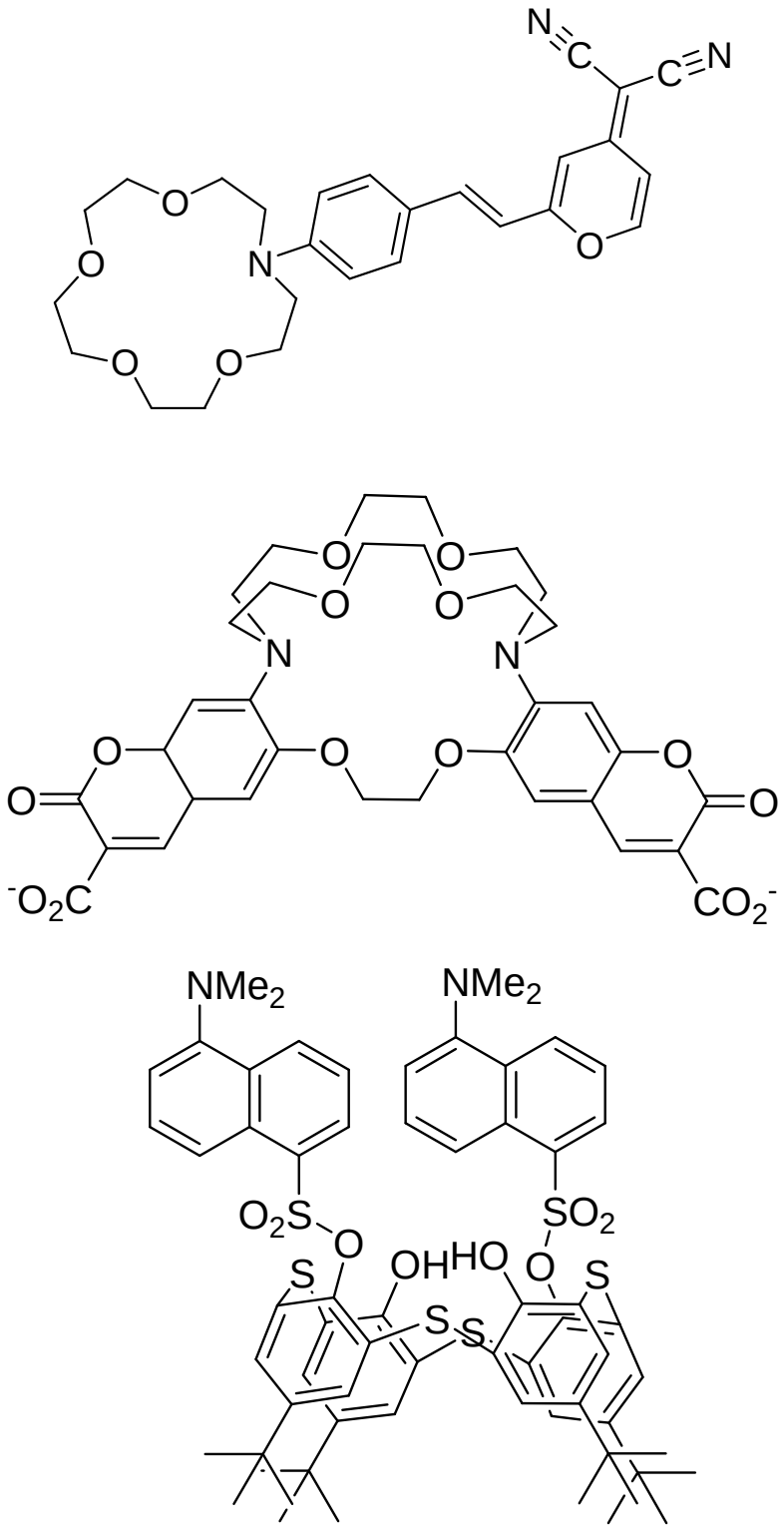

Figure 18 Examples for fluorescent ICT sensors in which cation binds to the electron donating group

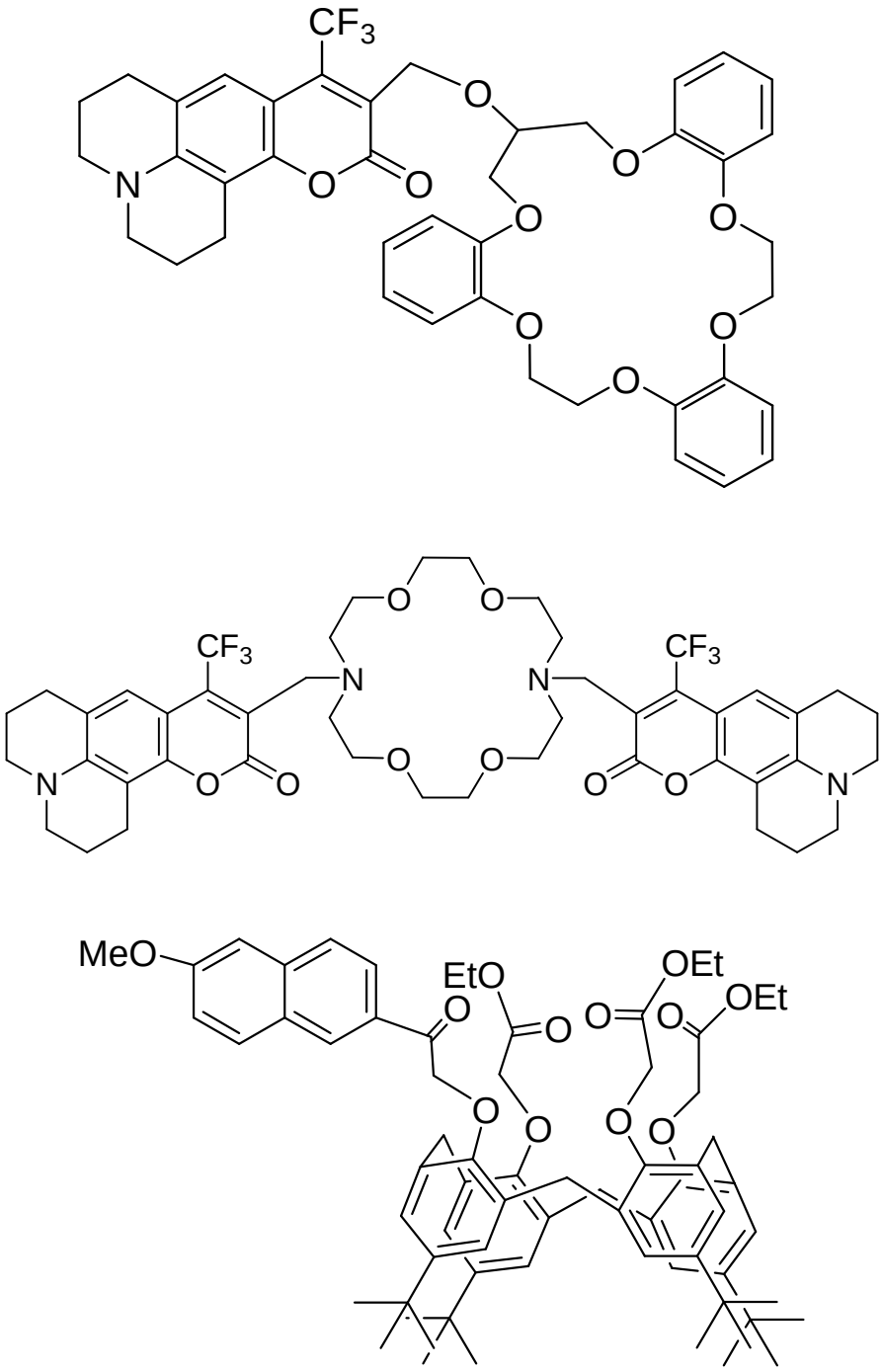

Figure 19 Examples for fluorescent ICT sensors in which cation binds to the electron accepting group

1.9. General Aspects of Boradiazaindacence (BODIPY)

The design and synthesis of original, fluorescent chemosensors for the measurement of analytically important ions and molecules continues to be an exciting area of research. In recent years, scientists have paid much attention on the synthesis of 4,4-difluoro-4-bora-3a,4a-diaza-*s*-indacene (difluoroborondipyrromethene, BODIPY, or BDP) based fluorescent probes, in which boradiazaindacene unit is created as a result of the chelation between dipyrromethene unit and BF_2 center, and their application as selective and efficient chemosensors **[13, 14]**. BODIPY derivatives can be obtained upon modification of the probe at carbon positions 1,3,5,7 and 8 (Figure 20) **[15]**.

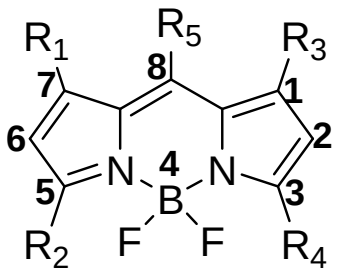

Figure 20 Carbon positions 1,3,5,7 and 8 on BODIPY

Popularity of BODIPY dyes arises from their narrow absorption and emission bands in the visible region of the spectrum, high absorption coefficient and fluorescence quantum yields, high molar extinction coefficient, the lack of ionic charge, which makes BODIPY dyes insensitive to solvent pH, and remarkably photostable **[15]**.

BODIPY derivatives are more hydrophobic than the commonly used 7-nitro-2,1,3-benzoxadiazol-4-yl (NBD) group, but less hydrophobic than pyrene. Unlike pyrene and NBD, the fluorescence emission of BODIPY dyes is relatively insensitive to environmental factors like medium polarity, pH, and oxygen **[16]**.

Moreover, BODIPY derivatives can be created by the attachment of aromatic polycycles (Figure 21). Illumination into the appended polycycle is followed by rapid intramolecular excitation energy transfer to the BODIPY. The pyrene derivative is strongly fluorescent and the net effect is to induce a large virtual Stokes' shift; this shift can reach as high as 10900 cm^{-1}. An important feature of these systems is that the two chromophores remain electronically isolated due to the orthogonal arrangement around the connecting linkage. The rate of energy transfer depends on the structure of the dual-dye system and decreases with increasing centre-to-centre separation in line with a dipole-dipole transfer mechanism **[17]**.

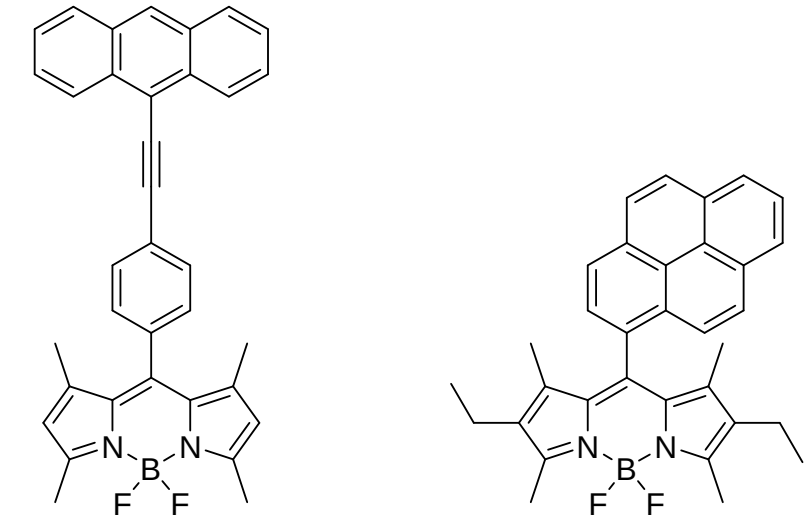

anthracene derivative pyrene derivative

Figure 21 Anthracene and pyrene derivatives of BODIPY.

Singlet energy transfer is both fast and highly directional in the derivatives of BODIPY created by the replacement of the F atoms with aryl or ethynylaryl subunits (Figure 22). This has led to the development of molecular dyads in which only the BODIPY unit fluoresces, even at low temperatures. Tuning the rate constant for intramolecular energy-transfer becomes feasible by optimization of the spectral overlap integral between fluorescence from the appendage and absorption by the BODIPY residue **[17]**.

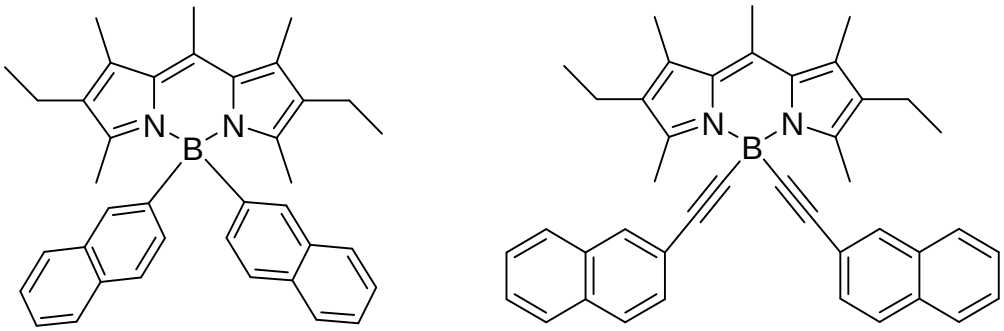

Figure 22 Structure of BODIPY with aryl and ethynylaryl subunits instead of F atoms.

An important issue concerning the design of novel fluorescent labels is to address the problem of Stokes' shifts which are small in most organic dyes. The common approach to enhancement of Stokes' shifts is to unite two chromophores in one molecule, one taking the role of energy donor and the other being the acceptor. In such tandem systems, a through space energy transfer process is believed to occur and this requires a significant overlap of the donor emission and acceptor absorption spectra, a requirement which determines the virtual Stokes' shifts **[17]**.

The orange/red color of BODIPY dyes constructed from 2,4-dimethyl-3-ethyl-pyrrole or 2,4-dimethyl-pyrrole can be shifted to the blue or green regions by logical modification. This can be achieved either by

replacement of the methyl group at the ortho-N position with styryl groups (Figure 23).

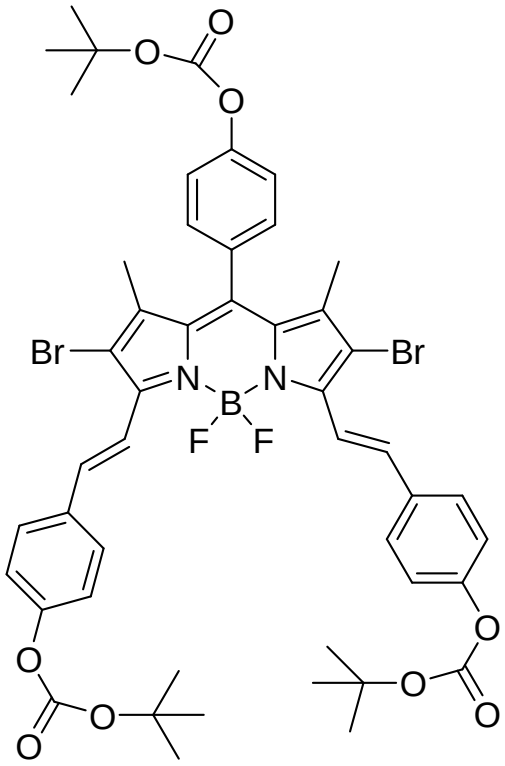

Figure 23 Replacement of the methyl groups with styryl groups

Consequently, numerous derivatives of BODIPY can be made by various substitutions which change their spectral properties; hence these dyes are so attractive. Also, our research group has great interest in these dyes. Various derivatives of BODIPYs that may have different applications such as light harvesting molecules, chemosensors, or photosensitizers are studied in our group. Light harvesting ability can be observed in a system of tetrakis(boron-dipyrrin) (BODIPY) appended perylenediimide (PDI) that was synthesized in our laboratory **[18]**. Furthermore chemosensor ability was conferred BODIPY molecule by suitable modifications; consequently it could sense a specific cation or anion. A novel chemosensor for phosphate anion was also synthesized

in our research group **[19]**. Moreover, photosensitizer ability could have a vital importance due to the usage in photodynamic therapy, which is a noninvasive method of treating malignant tumors and age-related macular degeneration, and is particularly promising in the treatment of multidrug-resistant (MDR) tumors. A BODIPY derivative as efficient photosensitizer was also synthesized in our laboratory **[20]**. As a result, the concept of BODIPY chromophore as a supramolecular building block is a new area of research direction, and our group is one of the pioneer groups and studies various applications of BODIPY.

1.10. Aim of the Study

In this project, our aim was to design and synthesize novel long wavelength emitting boradiazaindacences which can show opposite spectral shift in response to the same external stimulus.

CHAPTER 2

EXPERIMENTAL

2.1. Instrumentation

In this study characterization and analysis of the compounds were done by the Nuclear Magnetic Resonance Spectroscopy (NMR), Ultra-Violet/Visible Absorbance Spectroscopy and Fluorescence Emission Spectroscopy.

Bruker Gmbh DPX-400, 400 MHz High Performance Digital FT-NMR spectrometer at METU Chemistry Department NMR Laboratory, recorded ^{1}H and ^{13}C-Nuclear Magnetic Resonance Spectra of the synthesized compounds. $CDCl_3$ was used as NMR solvent, tetramethylsilane was the internal reference and ppm scale was used to designate the chemical shifts δ. Chemical shift multiplicities were recorded as s (singlet), d (doublet), t (triplet), q (quartet) and m (multiplet).

Varian Bio 100 UV/Vis Spectrophotometer was used to record Ultra-Violet/Visible Absorbance spectrum. For the Fluorescence Emission data Varian Cary Eclipse Fluorescence Spectrophotometer is used. During absorbance and emission analysis Sigma Spectrophotometer Silica (Quartz) cuvettes with 10 mm light path were used.

The characterization of the compound **8** was also done by the X-Ray Diffraction. Data were collected on an ENRAF NONIUS-CAD4 diffractometer with CuKα radiation (λ = 1.54184 Å). The cell parameters were determined from a least-squares refinement of 16 centered reflections in the range of $17.88 \leq \theta \leq 42.31°$. Data processing was accomplished with the CAD4 EXPRESS processing program. Data reduction was carried out using XCAD4. A psi-scan absorption correction was applied. The structure was solved by direct methods and refined by full-matrix least-squares on F^2 using the SHELXS97 and SHELXL97 software, respectively. All the non-hydrogen atoms were refined anisotropically.

The spectral and fluorescence decay measurements were carried out with the TM-3 laser-based fluorescence lifetime spectrometer equipped with the T-2A steady-state option. The TM-3 lifetime instrument utilized the GL-3300 nitrogen laser pumping the GL-302 high-resolution dye laser. The decay curves were measured with the spectroscopic detection technique.

Finally, the mass spectrometer analyses were also studied at the mass spectrometry research laboratory in Hacettepe University, Department of Chemistry. Matrix-assisted laser desorption/ionization (MALDI) mass spectrometry experiments were performed on a Applied Biosystems Voyager DE™ PRO mass spectrometer with delayed extraction. Samples were irradiated with a nitrogen laser (Laser Science Inc.) operated at 337nm and the laser beam was attenuated by a variable attenuator and focused on the sample target. Ions produced in the ion source were accelerated with a deflection voltage of 30,000 V. The ions were then differentiated according to their m/z using a time-of-flight mass analyzer or the time-of-flight reflectron mass analyzer.

2,4-dimethylpyrrole, boron trifluoride-diethyl etherate (BF_3OEt_2), 4-dimethylamino-benzaldehyde, 4-pyridine carboxaldehyde and N-Bromosuccinimide (NBS) were purchased from Sigma & Aldrich in 97, 100, 99, 97 and 99% purity, respectively. 2,2'-Azobis(2-methylpropionitrile) (AIBN) was obtained from Fluka in ≥ 98% purity. NEt_3, benzoyl chloride, and CCl_4 were obtained from MERCK-Schuchardt in ≥ 99% purity. CH_2Cl_2 and AcOH were purchased from Carlo Erba in 99 and 99.5% purity, respectively. Piperidine was obtained from Avocado, benzene from Riedel-de Hoen in 99 and 99.8% purity, respectively. Chloroform, hexane and ethylacetate were distilled over $CaCl_2$ before using. NMR solvent, $CDCl_3$, was obtained from Merck KGaA in 98.9% purity. Column chromatography off all products was performed by using Merck Silica Gel 60 (particle size: 0.063-0.2 mm, 70-230 mesh ASTM) as stationary phase. Reactions were monitored by thin layer chromatography using Merck Silica Gel 60 F_{254} TLC Aluminium Sheets 20x20 cm.

2.2. Synthesis of the 1,3,5,7-tetramethyl-8-phenyl-4-4'-difluoroboradiazaindacene(3)

Synthesis of this BODIPY derivative was carried out according to the following procedure **[22]**. 2,4-dimethylpyrrole (**1**, 1.5 g, 15.77 mmol) and benzoyl chloride (**2**, 1.108 g, 7.88 mmol) were dissolved in CH_2Cl_2 in which N_2 was passed previously for 15 minutes. Reaction mixture was refluxed for 24 hours. After cooling NEt_3 (5.255 g, 51.9 mmol) and BF_3OEt_2 (3.376 g, 23.8 mmol) were added, respectively, and refluxed again for 24 hours. The resulting mixture was then washed three times with H_2O. Organic phase was collected, dried over Na_2SO_4 and

evaporated to dryness. The residue was chromatographed on silica gel ($CHCl_3$) (yield: 24%) (Figure 24).

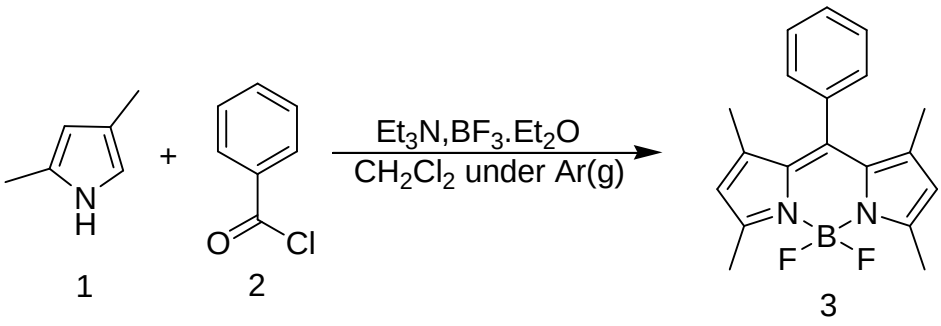

Figure 24 Synthesis of 1,3,5,7-tetramethyl-8-phenyl-4-4'-difluoroboradiazaindacence (**3**)

2.3. Synthesis of dimethylaminostyryl derivative of BODIPY (5)

8-phenyl-BODIPY (**3**, 0.260 g, 0.802 mmol) and 4-(dimethylamino)-benzaldehyde (**4**, 0.479 g, 3.208 mmol) were dissolved in minimum amount of benzene. Piperidine (0.683 mL) and acetic acid (0.567 mL) were added. The reaction mixture is refluxed for 26 hours (monitoring is done by TLC) in the presence of Dean-Stark apparatus. After the reaction is complete, solvent is removed under vacuum and the purification is done by column chromatography (Hexane: $CHCl_3$, 1:4) (yield: 90%) (Figure 25).

^{1}H NMR (400 MHz, $CDCl_3$): 1.35 (s, 6H, CH_3), 2.95 (s, 12H, $N(CH_3)_2$), 6.52 (s, 2H, pyr-H), 6.65 (d, 4H, *J*=8.0 Hz), 7.11 (d, 2H, *J*=16. 2 Hz), 7.23-7.28 (m, 2H, Ar-H), 7.35-7.54 (m, 9H) (Figure 35).

^{13}C NMR (100 MHz, $CDCl_4$): 150.9, 137.9, 136.5, 129.1, 128.9, 128.3, 125.3, 117.1, 115.1, 112.2, 40.3 (Figure 36).

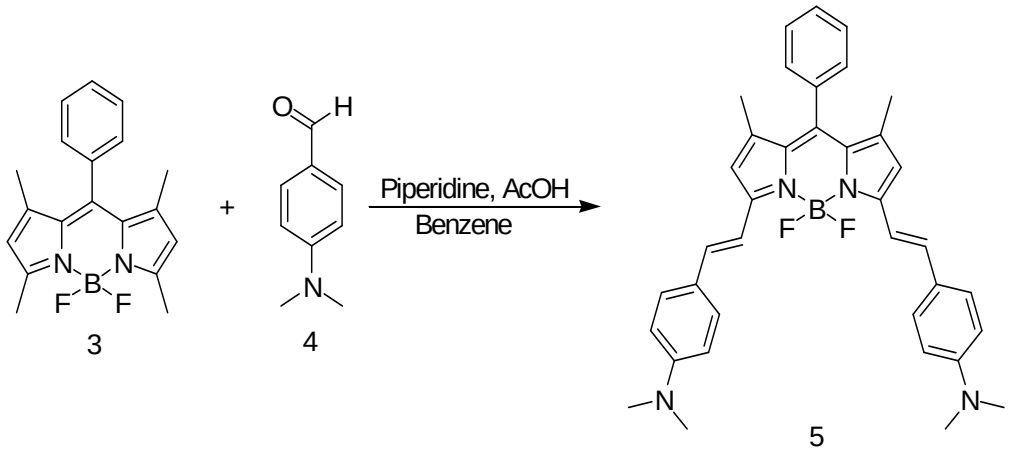

Figure 25 Synthesis of dimethylaminostyryl derivative of BODIPY(**5**)

2.4. Synthesis of the 2,6-dibromo-1,3,5,7-tetramethyl-8-phenyl-4,4'-difluoroboradiazaindacene(6)

8-phenyl-BODIPY (3, 0.33 g, 1.02 mmol), AIBN (0.335 g, 2.04 mmol), and NBS (0.363 g, 2.04 mmol) were refluxed for 30 min in CCl_4 (15 mL). Crude product was then concentrated under vacuum, and purified by silica gel column chromatography (Hexane: EtOAc, 3:1) (yield: 80%) (Figure 26) **[21]**.

^{1}H NMR (400 MHz, $CDCl_3$): 1.37 (s, 6H, CH_3), 2.56 (s, 6H, CH_3), 7.15-7.2 (m, 2H, Ar-H), 7.42-7.48 (m, 3H, Ar-H) (Figure 37).

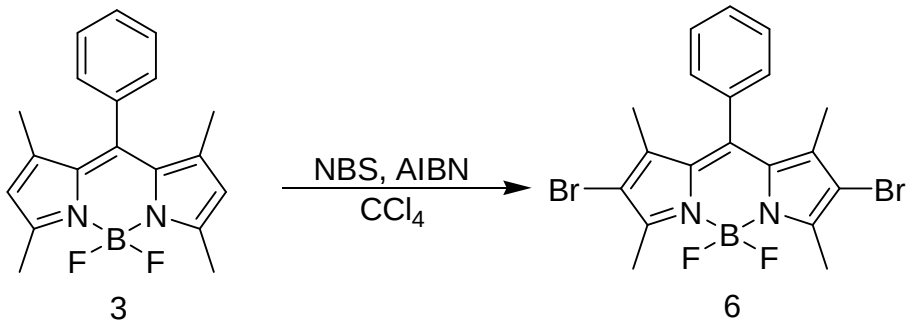

Figure 26 Synthesis of the 2,6-dibromo-1,3,5,7-tetramethyl-8-phenyl-4,4'-difluoroboradiazaindacene (**6**)

2.5. Synthesis of pyridyl derivative of BODIPY (8)

A procedure was applied that was very similar to the synthesis of dimethylamino derivative of BODIPY. Thus, dibromo-8-phenyl-BODIPY (**6**, 0.200 g, 0.617 mmol), isonicotinealdehyde (**7**, 0.264 g, 2.47 mmol), piperidine (0.525 mL) and acetic acid (0.436 mL) were used in this reaction. Again the reaction was carried out in the presence of Dean-Stark apparatus. The residue was chromatographed on silica gel (yield: 94%) (Figure 27).

^{1}H NMR (400 MHz, $CDCl_3$): 1.39 (s, 6H, CH_3), 7.23-7.26 (m, 2H, Ar-H), 7.44 (d, 4H, J=5.5 Hz) 7.49-7.53 (m, 3H, Ar-H), 7.80 (d, 2H, *J*=16.7 Hz), 7.97 (d, 2H, *J*=16.7 Hz) 8.61 (d, 4H, J= 4.8 Hz, Ar-H) (Figure 38).

^{13}C NMR (100 MHz, $CDCl_3$): 149.4, 142.8, 141.4, 135.4, 133.2, 131.8, 129.0, 128.7, 126.9, 122.1, 121.0, 120.5, 115.7, 113.6, 13.1 (Figure 39).

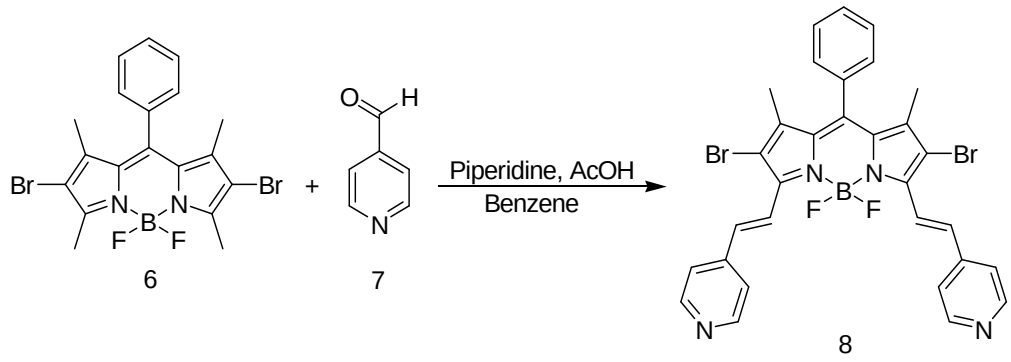

Figure 27 Synthesis of pyridyl derivative of BODIPY (**8**)

CHAPTER 3

RESULTS AND DISCUSSION

There is no doubt that supramolecular chemistry has a significant importance in the determination of ions. In other words, scientists are searching an effortless way to detect ions that are vital in environmental and health issues, instead of analyzing them by AAS, AES or other instrumental techniques. Supramolecular chemistry offers an alternative technique, fluorescence sensors. The medium in which the fluorescent sensor exists has a certain color in the lack of specific ion but changes its color in the presence of this ion. This technique functions according to certain photophysical mechanisms, such as PET and ICT. In our study, ICT mechanism can be easily observed.

3.1. Synthesis of fluorescent molecules which are sensitive to H^+ ion

Initially, reaction pathways are decided according to the target molecules, **5** and **8**. First step is the synthesis of 8-phenyl-BODIPY, **3**. Corresponding aldehydes are generally used to synthesize BODIPY dyes. Another method to synthesize these dyes is to use corresponding acyl chlorides. In our case, benzoyl chloride reacts with two equivalents of 2,4-dimethylpyrrole. The crude product is purified as pure 8-phenyl-BODIPY by chromatographic methods.

The yield in the synthesis of BODIPY dyes has a low value, in the range of 20-25% approximately.

For the target molecule **5**, synthesis of 8-phenyl-BODIPY is followed by condensation reaction with 4-(dimethylamino)-benzaldehyde, **4**, in the presence of piperidine and acetic acid in order to reach dimethylamino derivative of BODIPY. After chromatographic separation doubly styryl substituted BODIPY dye, **5**, is mainly obtained.

For the target molecule **8**, the reaction with 4-pyridinecarboxaldehyde did not proceed at all, under the same conditions. Based on previous observations, to increase the acidity of the methyl groups, bromination of compound **3** at 2 and 6 positions was then carried out in the presence of NBS and AIBN, as it was shown in our group that this improves the chances of aldol condensation. This is then followed by condensation reaction with pyridine-4-carboxaldehyde, **7**, in the presence of piperidine and acetic acid after which purification is done by column chromatography that gives doubly styryl substituted BODIPY dye, **8**.

In the synthesis of both compound **5** and **8**, the Dean-Stark apparatus was used in order to remove water azeotropically during reflux.

3.2. Characterization of BODIPY Dyes

Characterization of all molecules is done by NMR spectroscopy. Furthermore, the X-ray structure of pyridyl derivative, **8**, was obtained at

Department of Physics Engineering, Hacettepe University, Beytepe, Ankara, Turkey (Figure 28).

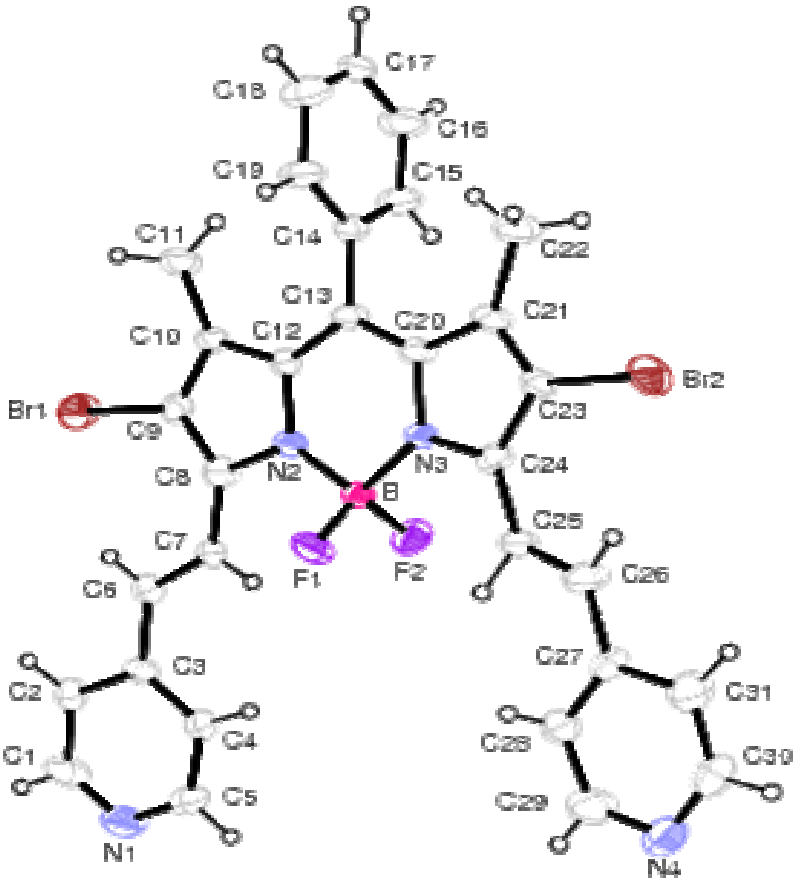

Figure 28 X-Ray structure of compound 8

The spectrum proves that the phenyl group at 8th position is orthogonal to the BODIPY plane as expected. In the complex the plane defined by the atoms F1-B-F2 and plane of the phenyl ring are almost perpendicular to the plane defined by the other atoms of the molecule (the dihedral angles are 85.7 (2) and 88.6(3)°, respectively).

Crystal data for compound **8**: $C_{31}H_{23}BBr_2F_2N_4$; *M*= 660.14 g mol^{-1}; triclinic; $P\bar{1}$; *a*= 8.520(2) Å, *b*= 12.605(2) Å, *c*= 12.968(2) Å, α =92.105(13)°, β=97.360(16)°, γ=95.410(14)°; *V*= 1373.4(4) Å^3 ;

Z= 2; *T*= 293(2) K; 3.44 ≤ θ ≤ 70.14°. A total of 4744 reflections collected, 4451 independent reflections; *R*1= 0.0722, wR2 = 0.1592 for 1839 reflections with *I* > 2σ(*I*) and *R*1 = 0.2252, wR2 = 0.2173 for all data; CCDC-645483 (Figure 29).

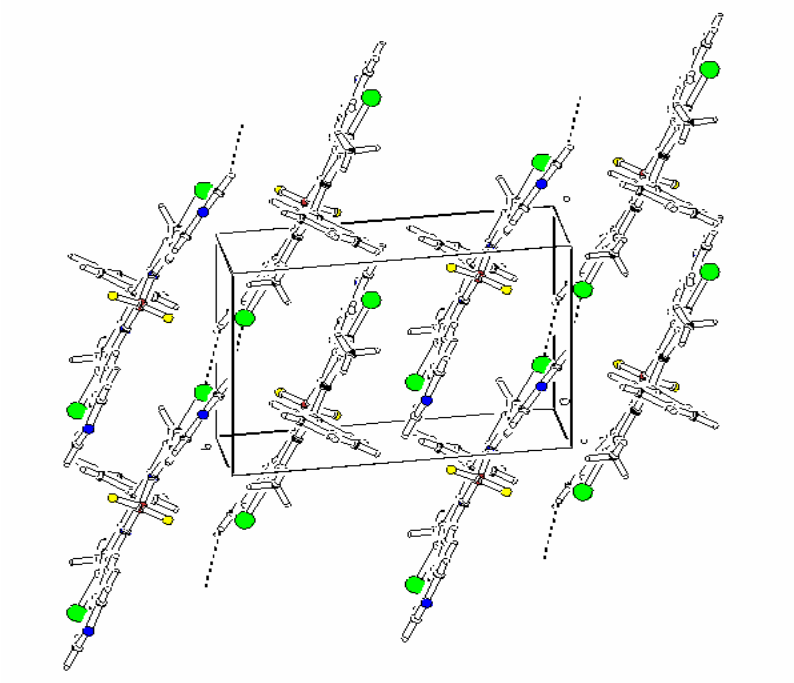

Figure 29 Crystal structure of compound **8**

Inter and intra hydrogen bond parameters are shown in the table 1. Moreover, the hydrogen bond is formed between the bromine atom of one molecule and the hydrogen atom of the other molecule (Figure 30).

Table 1 Inter and intra hydrogen bond parameters

Donor	Acceptor	D–H (Å)	H•••A (Å)	D–A (Å)	D–H•••A(°)
C2	Br1^{I}	0.93	2.86	3.600	138
C6	Br1	0.91	2.62	3.382	143
C7	F2	0.90	2.52	3.113	124
C26	Br2	0.90	2.60	3.391	147

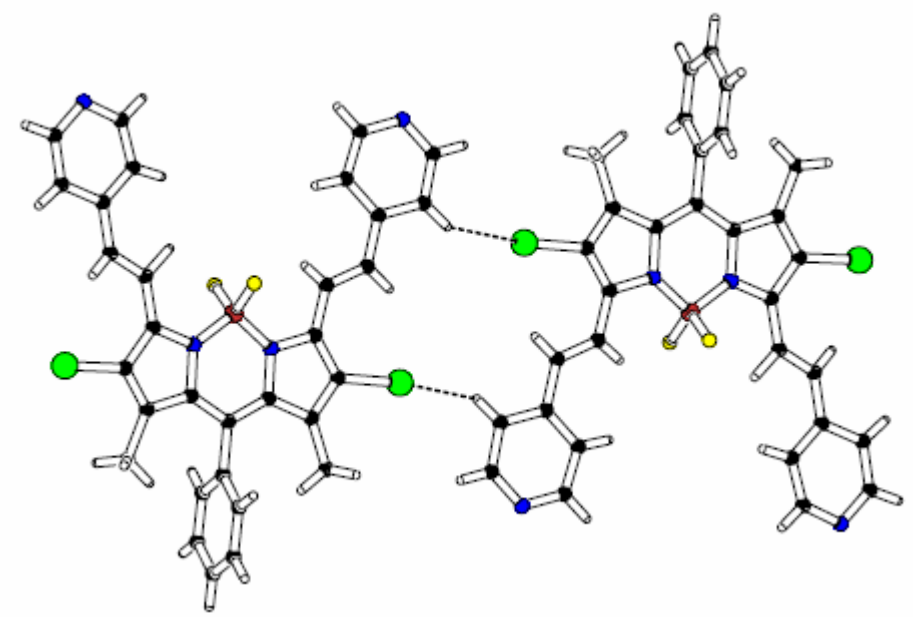

Figure 30 X-ray structure showing hydrogen bond formation between two molecules

3.3. Photophysical Properties of BODIPY Dyes

Boradiazaindacene dyes have fundamental properties such as high absorption coefficient and fluorescence quantum yields, high molar extinction coefficient, and remarkably photostability and they are insensitive to solvent pH due to the lack of ionic charge. These properties can be improved by modification of BODIPY.

In order to create fluorescent sensor, it is necessary to introduce electron donor or acceptor group into the BODIPY. These modification steps are explained previously. Photophysical properties of both

compounds **5** and **8** are studied to examine whether they show ICT properties and have acid switchable character, or not.

On one hand, compound **5** shows two separated protonation events by the addition of TFA to a dichloromethane solution. This in accordance with earlier reports in literature for bis(dimethylaminophenyl)aza-BODIPY dyes **[22]**. Therefore, on gradual addition of TFA, the long wavelength peak decreases with concomitant rise of a peak at 620 nm. This peak can be assigned to the monoprotonated species. Further addition, as expected, results in a decrease of absorption at this wavelength, though a new peak at 580 nm becomes prominent. This peak is due to the diprotonated species (Figure31). Emission spectra show similar changes in the absorption spectra. Hence, three different protonation states cause three different states of absorption and emission spectra. The corresponding emission peaks for **5**, **5**-H^+ and **5**-$2H^+$ are 750, 630 and 570 nm, respectively. A blue shift on the addition of TFA is expected due to the dimethylamino substituent considering that as an ICT donor group. Dimethylamino functionality becomes considerably less effective electron donor on protonation, and this causes a blue shift (Figure 32).

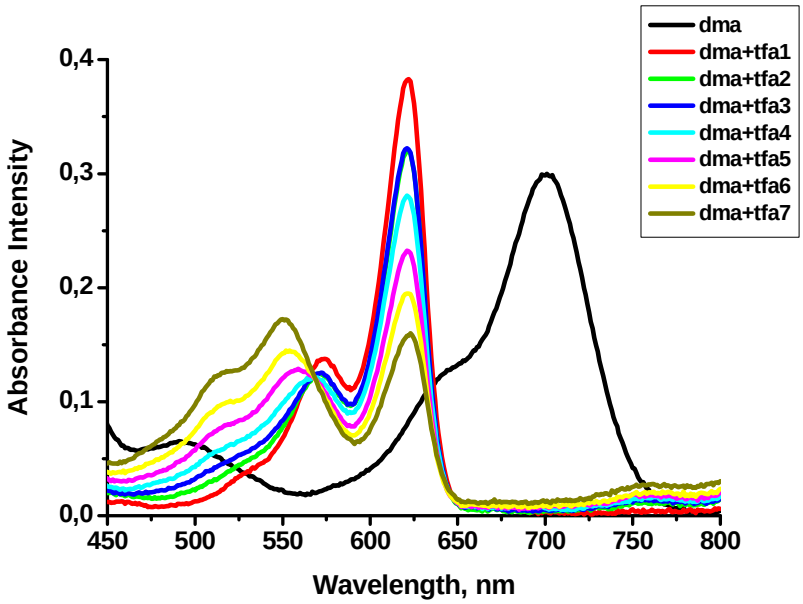

Figure 31 Absorption spectrum of compound **5**

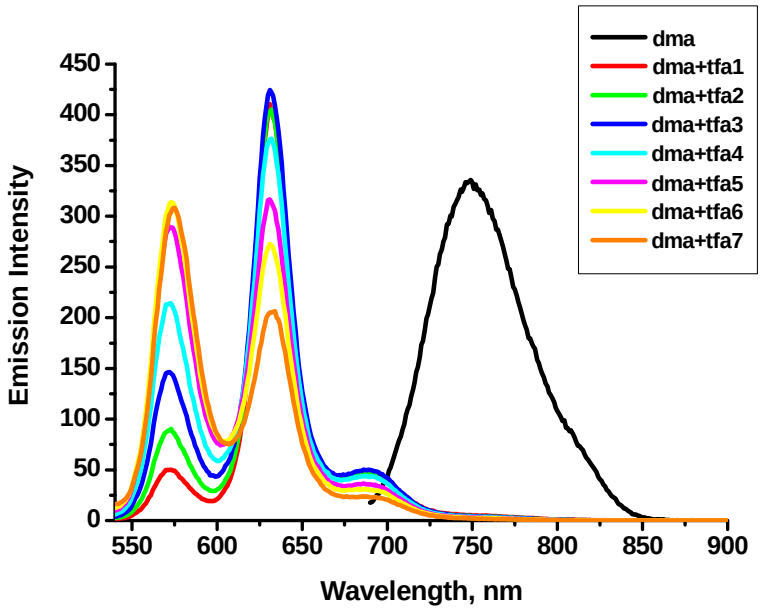

Figure 32 Emission spectrum of compound **5**

On the other hand, compound **8** shows a different behavior. The gradual addition of a small amount of TFA results in a single distinct spectrum. So it seems like the pyridine group is more basic than dimethylamino and both pyridyl nitrogens are protonated in one step. The absorption peak at 620 nm shifts to 660 nm on TFA addition (Figure 33). This red shift is not surprising since the pyridyl groups are electron withdrawing substituents for ICT mechanism, in such fluorophores it is known that any event making the electron acceptor stronger (like protonation or cation binding) produces an auxochromic change that is an increase in the extinction coefficient and a red shift in the emission spectrum. The emission spectrum also shows just one peak at 675 nm on TFA addition (Figure 34).

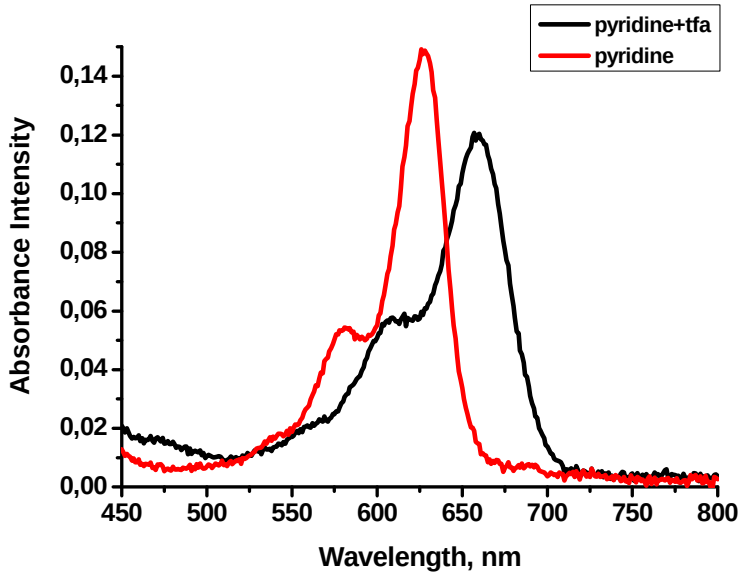

Figure 33 Absorption spectrum of compound **8**

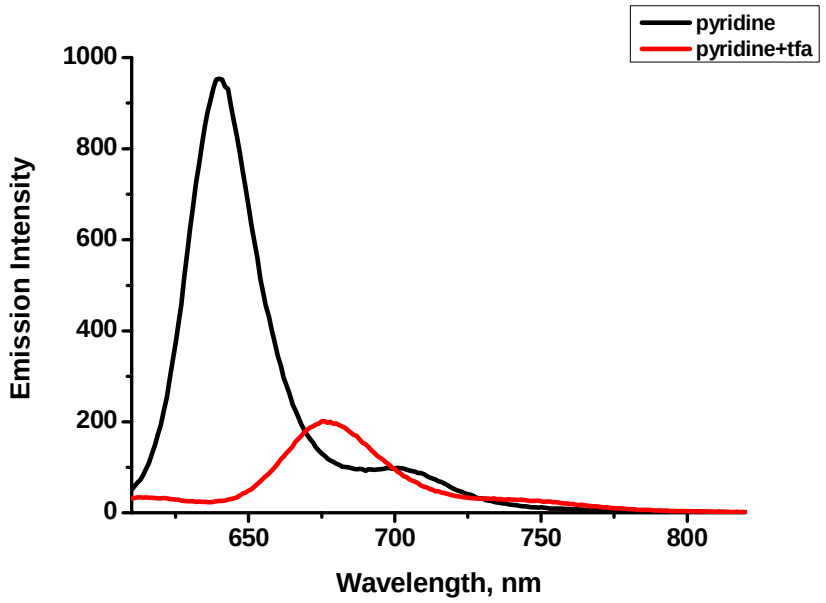

Figure 34 Emission spectrum of compound **8**

3.4. Fluorescence Decay Measurements

Time resolved fluorescence spectroscopy reveals emissive species with different lifetimes. Pyridyl derivative **8**, shows a single exponential decay with a lifetime of 4.29 ns (Figure 40). The protonated (doubly) species (**8**+2H^{+}) has a shorter lifetime of 3.06 ns, which is an accordance with a general principle of bathochromic shifts increasing non-radiative rate constants (Figure 41).

On the other hand, protonation of the dimethylaminophenyl derivative is stepwise as indicated earlier, and **5** has an emissive lifetime of 2.7 ns (Figure 42). When a very small aliquot of TFA was added (10μL) while

the original emission disappears, two new emissive species, **5**+H^+ and **5**+$2H^+$ become prominant. The emission lifetimes are 1.20 and 3.6 ns, respectively (Figure 43). When much larger amounts of TFA were added, short lifetime emission (assigned to **5**+H^+) disappeared and only the emission collected has a lifetime of 3.4 ns (Figure 44).

3.5. Mass Spectrometry Analysis

Mass spectrometry analysis were done at the mass spectrometry research laboratory in Hacettepe University, Department of Chemistry. MALDI spectroscopy of the pyridyl-derivative yielded two prominent peaks, corresponding to $[M+H]^+$ (661.19 m/e) and $[M+H-F]^+$ (642.13). Dimethylamino derivative resulted in a molecular ion at 586.5 (M^+) and $[M-F]^+$ peak at 567.5 m/e.

CHAPTER 4

CONCLUSION

In this study, we synthesized novel BODIPY dyes as fluorophores whose absorption and emission spectra are located at the long wavelength region of the visible spectrum. Our synthesis strategy was one that could yield fluorophores which show opposite spectral changes when introduced to the same stimulus. We have succeeded in this, by synthesizing a pyridyl and dimethylaminophenyl substituted extended conjugation boradiazaindacene dyes. These dyes can be excited in the red region (630-680) and their emission peaks are further towards the near IR region.

The fact that these two targeted dyes can be modulated in two directions by a single affector is important for the following reasons:

a) Fundamental photophysical processes were shown to be modulated at will.
b) Novel chemosensor for pH (hydrogen ion) and or other cations can be designed.
c) Molecular logic gates can be built upon these new boradiazaindacene platforms.
d) Photodynamic activity of these dyes can be altered by pH modulation.

The structures of new obtained fluorophores were examined with ^{1}H and ^{13}C-NMR, mass spectroscopy and crystallographic analysis. The changes in spectral properties were studied with steady-state and time-resolved fluorescence spectroscopy were shown to be in accordance with acid-base equilibria. Further work along these lines is expected to yield promising molecular devices.

REFERENCES

[1] Atwood, J.L. and Steed, J.W., *Encyclopedia of Supramolecular Chemistry*, Marcel Dekker, New York, 2004

[2] Lehn, J.M., Angew. Chem. Int. Ed. Engl., 1988, 27, 89

[3] Lehn, J.M., Pure Appl. Chem., 1978, 50, 871

[4] Beer, P.D., Gale P.A. and Smith D.K., *Supramolecular Chemistry*, Oxford, 1999

[5] Lehn, J.M., *Supramolecular Chemistry*, VCH, Germany, 1995

[6] Müller-Dethlefs, K., Hobza, P., Chem. Rev., 2000, 100, 143

[7] Atwood, J.L. and Steed, J.W., *Supramolecular Chemistry*, John Wiley & Sons, England, 2000

[8] Lakowicz J.R., *Principles of Fluorescence Spectroscopy*, Plenum Press, New York, 1983

[9] Skoog, D.A., Holler, F.J., Nieman, T.A., *Principles of Instrumental Analysis,* Harcourt Brace & Company, USA, 1998

[10] Valeur, B., Leray, I., Coor. Chem. Rev., 2000, 205, 3

[11] de Silva, A.P., Gunaratne, H.Q.N., Gunnlaugsson, T., Huxley, A.J.M., McCoy, C.P., Rademacher, J.T., Rice, T.E., Chem. Rev. 1997, 97, 1515

[12] Callan, J.F., de Silva, A.P., Magri, D.C., Tetrahedron, 2005, 61, 8551

[13] Boens, N., Baruah, M., Qin, W., Flors, C., Hofkens, J., Vallée, R.A.L., Beljonne, D., Van der Auweraer, M., De Borggraeve, W.M., J. Phys. Chem. A. 2006, 110, 5998

[14] Ziessel, R., Goze, C., Ulrich, G., Org. Let., 2006, 8, 20, 4445

[15] Brennan, J.D., Tleugabulova, D., Zhang, Z., J. Phys. Chem. B, 2002, 106, 13133

[16] Brockman, H.L., Dahim, M., Mizuno, N.K., Li, X.M., Momsen, W.E., Momsen, M.M., Biophysical Journal, 2002, 83, 1511

[17] Ziessel, R., Ulrich, G., Harriman, A., New J. Chem., DOI: 10.1039/b617972j

[18] Akkaya, E.U., Yilmaz, M.D., Bozdemir, O.A., Organic Letters, 2006, 8, 2871

[19] Akkaya, E.U., Coskun, A., Baytekin, B.T., Tetrahedron Letters, 2003, 44, 5649

[20] Akkaya, E.U., Atilgan, S., Ekmekçi, Z., Doğan, A.L., Guc, D., Chem. Commun., 2006, 4398

[21] Akkaya, E.U., Dost, Z., Atilgan, S., Tetrahedron, 2006, 62, 8484

[22] O'Shea, D.F., McDonnell S.O., Organic Letters, 2006, 8, 3493

APPENDIX

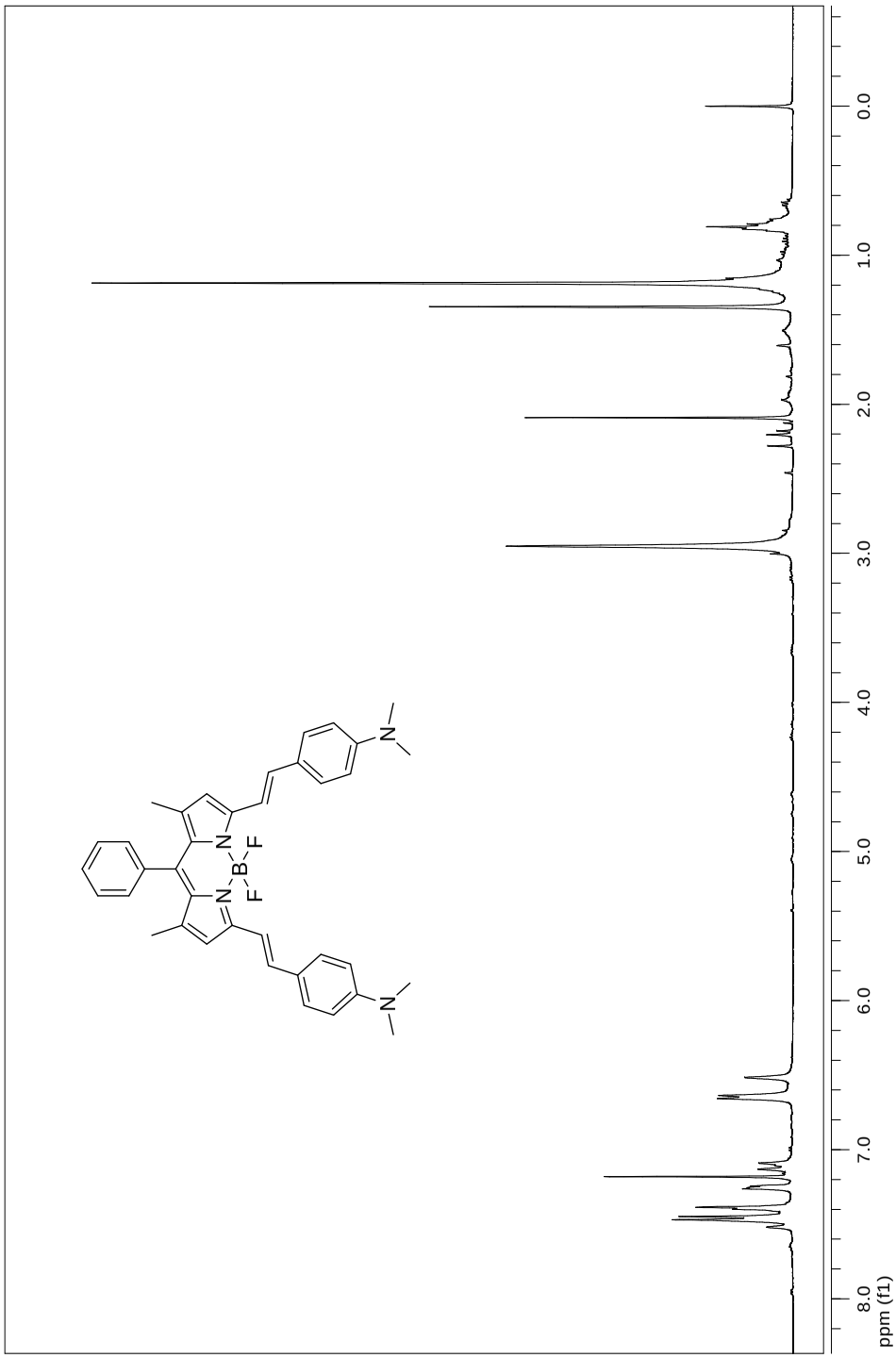

Figure 35 ^{1}H spectrum of compound 5

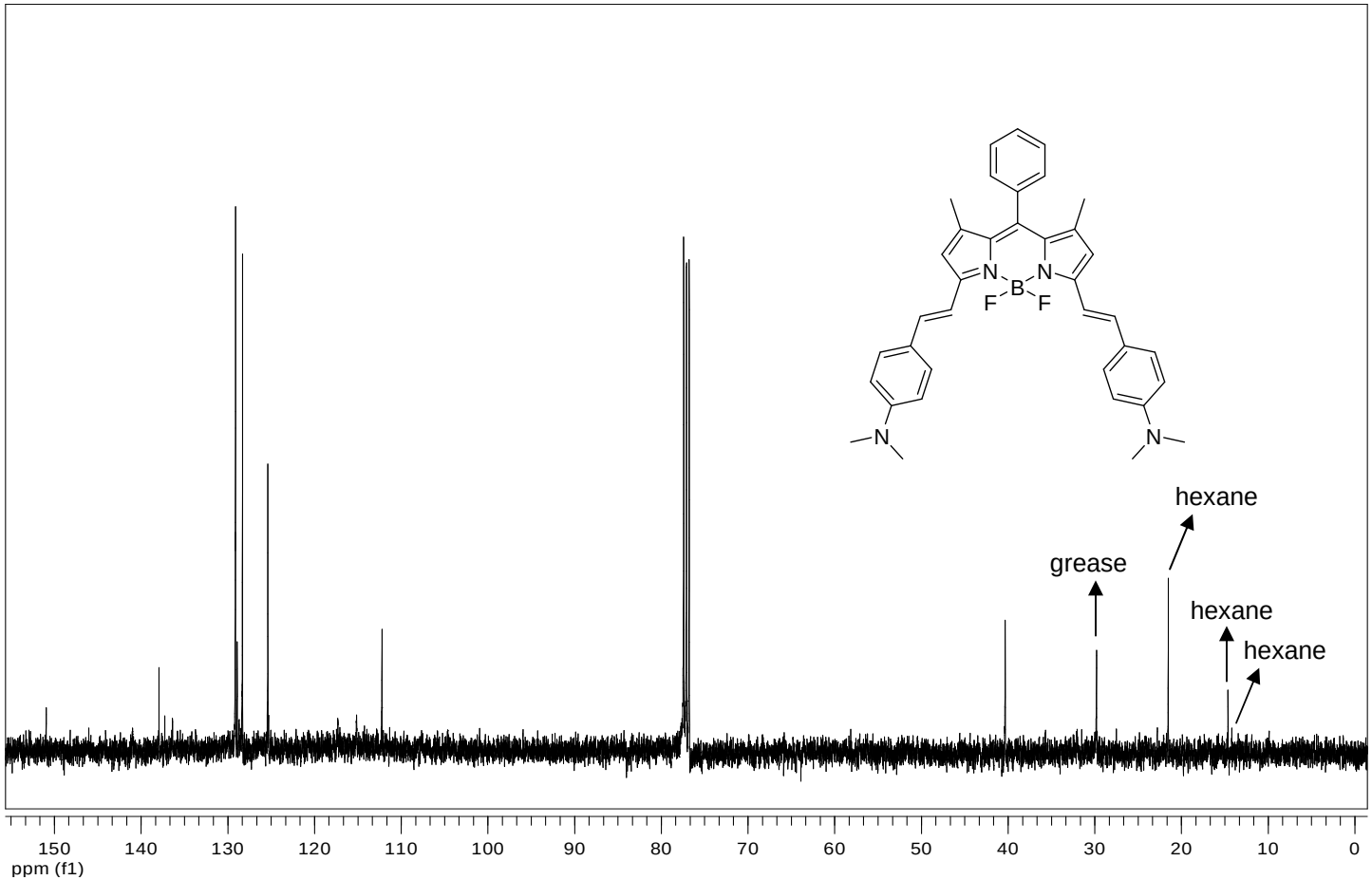

Figure 36 ^{13}C spectrum of compound 5

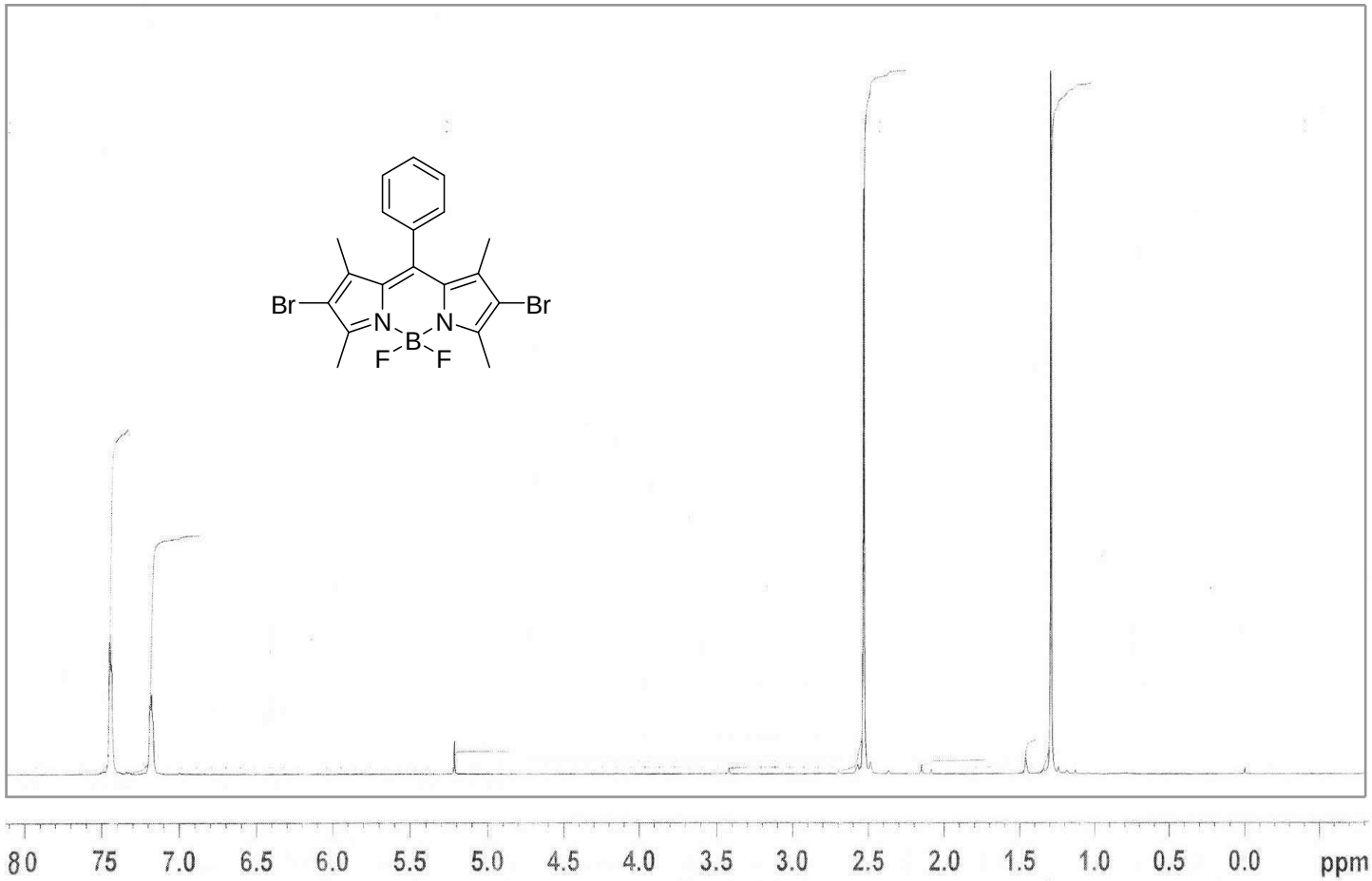

Figure 37 ^{1}H spectrum of compound 6

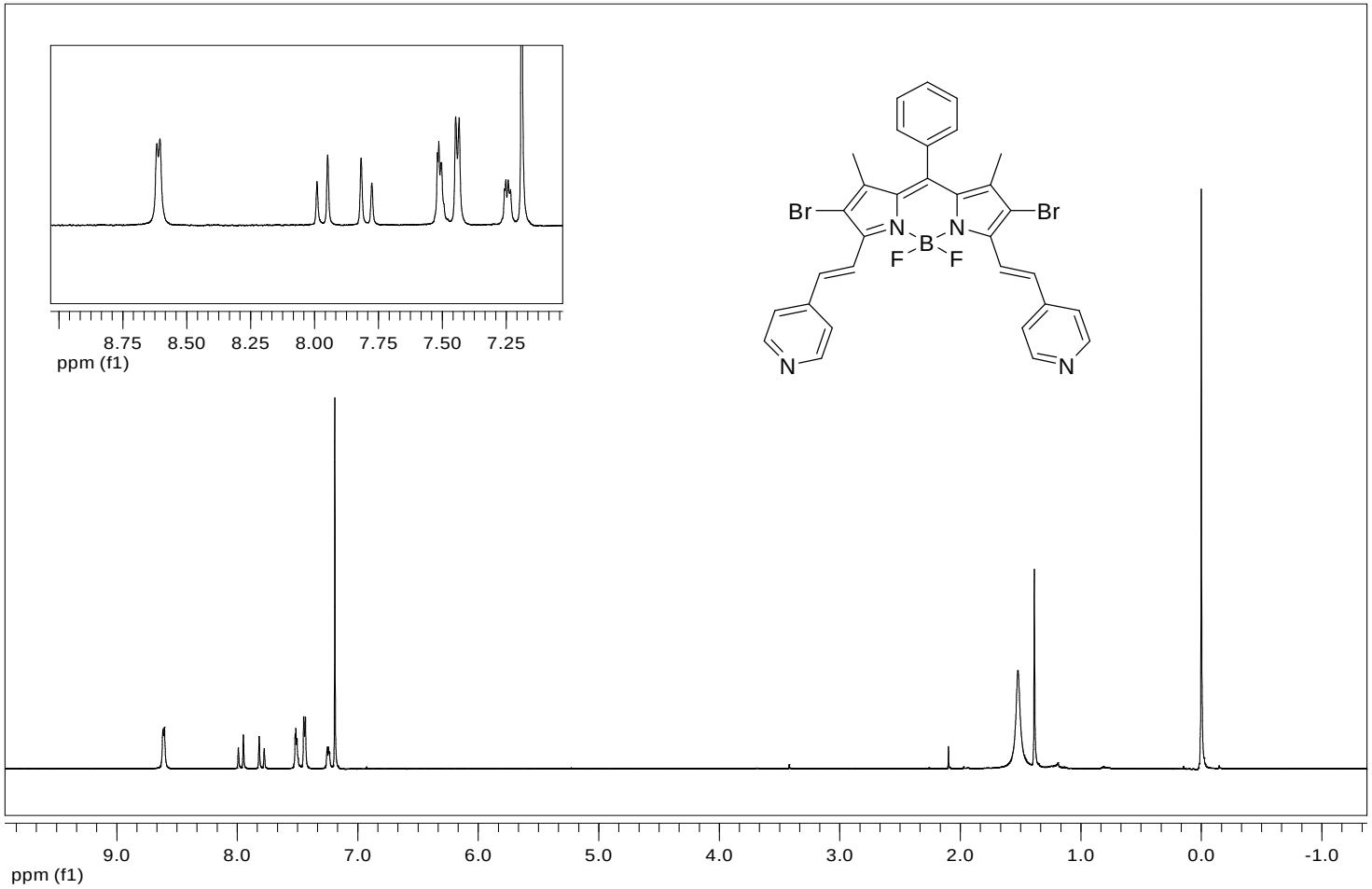

Figure 38 ^{1}H spectrum of compound 8

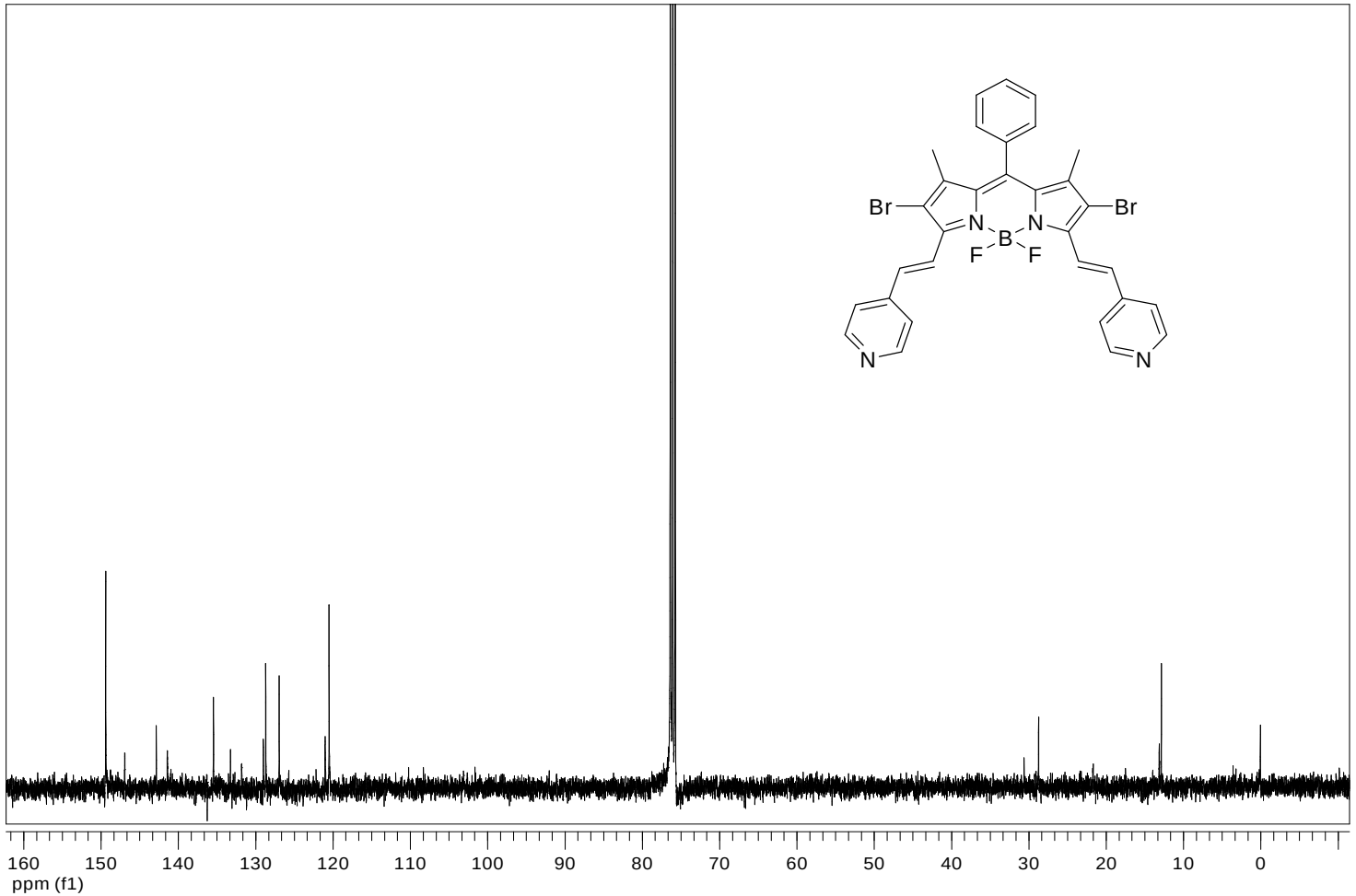

Figure 39 ^{13}C spectrum of compound 8

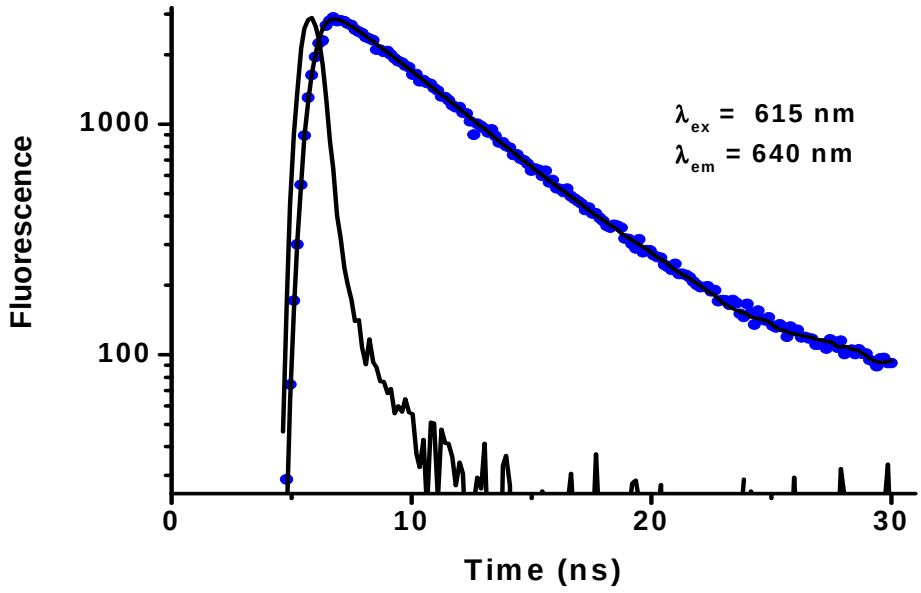

Figure 40 Fluorescence decay of compound 8 in $CHCl_3$. The recovered lifetime is 4.29 ns

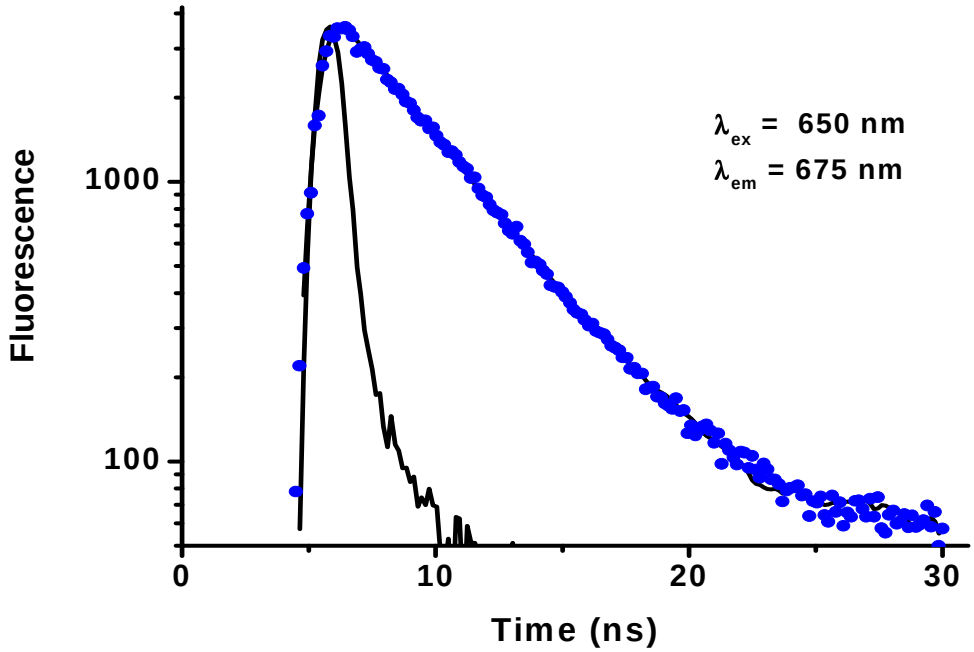

Figure 41 Fluorescence decay of compound 8 with 20 µL of TFA added to 3 mL of $CHCl_3$ solution. The recovered lifetimes is 3.06 ns

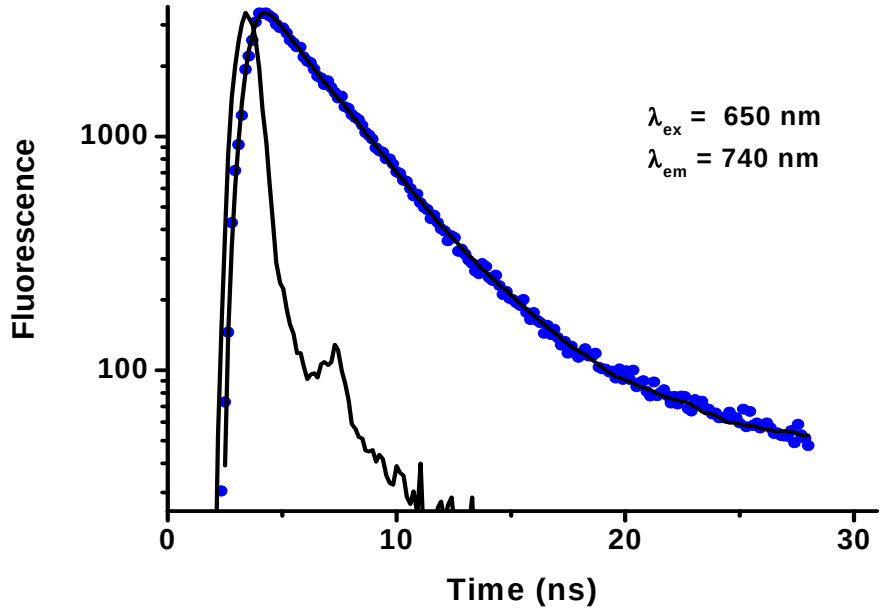

Figure 42 Fluorescence decay of compound 5 in $CHCl_3$. The recovered lifetimes are 2.7 ns (97%)

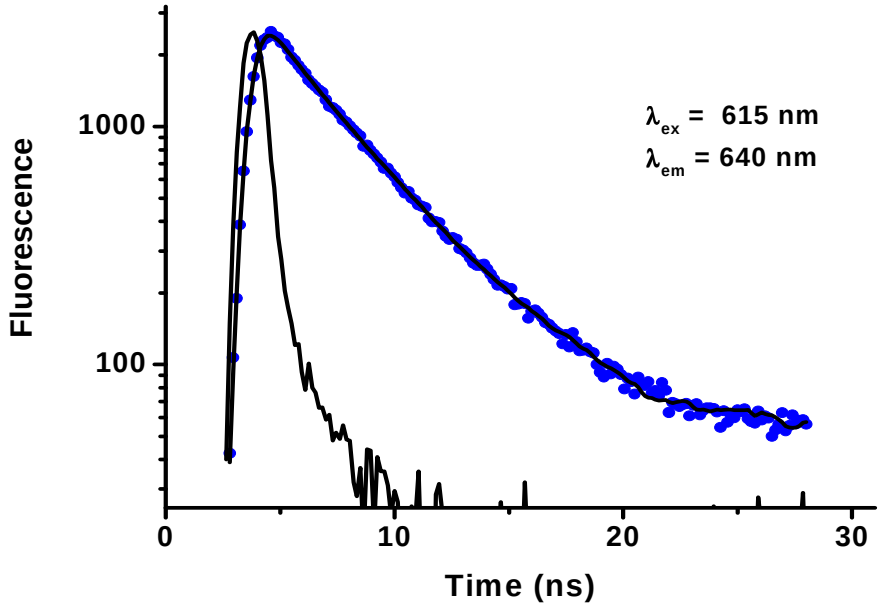

Figure 43 Fluorescence decay of compound 5 with 10 µL of TFA added to 3 mL of $CHCl_3$ solution. The recovered lifetimes are 3.6 ns (70%) and 1.20 ns (30%).

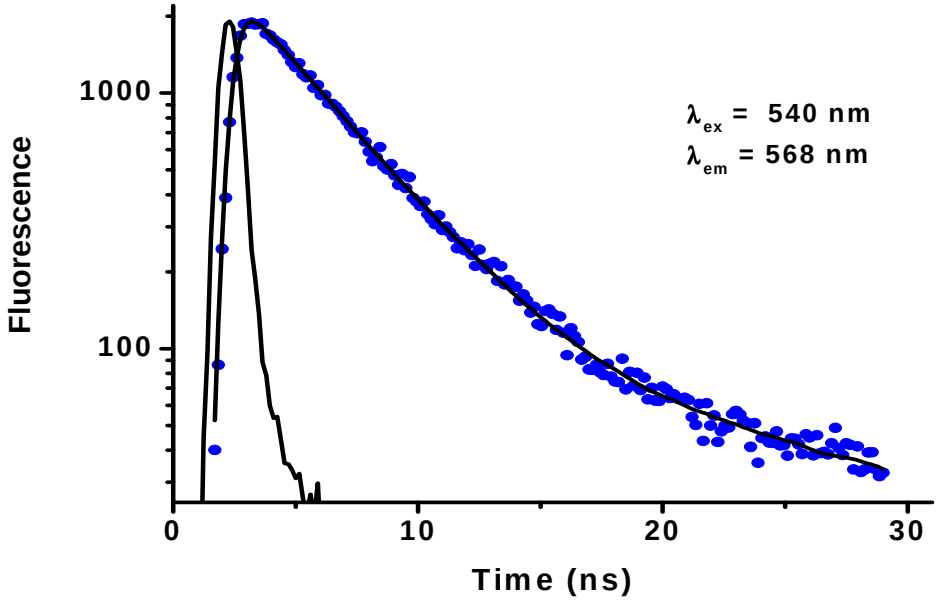

Figure 44 Fluorescence decay of compound 5 with 0.5 mL of TFA added to 3 mL of $CHCl_3$ solution. The recovered lifetimes are 3.4 ns (93%) and 8.3 ns (7%)